



Review

Current Trends in SPR Biosensing of SARS-CoV-2 Entry Inhibitors

Elba Mauriz ^{1,2,*}  and Laura M. Lechuga ³ 

¹ Department of Nursing and Physiotherapy, Campus de Vegazana, Universidad de León, s/n, 24071 León, Spain

² Institute of Food Science and Technology (ICTAL), La Serna 58, 24007 León, Spain

³ Nanobiosensors and Bioanalytical Applications Group, Catalan Institute of Nanoscience and Nanotechnology (ICN2), CSIC, BIST, and CIBER-BBN, Campus UAB, 08193 Barcelona, Spain; laura.lechuga@icn2.cat

* Correspondence: elba.mauriz@unileon.es; Tel.: +34-987-293617

Abstract: The emerging risk of viral diseases has triggered the search for preventive and therapeutic agents. Since the beginning of the COVID-19 pandemic, greater efforts have been devoted to investigating virus entry mechanisms into host cells. The feasibility of plasmonic sensing technologies for screening interactions of small molecules in real time, while providing the pharmacokinetic drug profiling of potential antiviral compounds, offers an advantageous approach over other biophysical methods. This review summarizes recent advancements in the drug discovery process of Severe Acute Respiratory Syndrome Coronavirus 2 (SARS-CoV-2) inhibitors using Surface Plasmon Resonance (SPR) biosensors. A variety of SPR assay formats are discussed according to the binding kinetics and drug efficacies of both natural products and repurposed drugs. Special attention has been given to the targeting of antiviral agents that block the receptor binding domain of the spike protein (RBD-S) and the main protease (3CLpro) of SARS-CoV-2. The functionality of plasmonic biosensors for high-throughput screening of entry virus inhibitors was also reviewed taking into account experimental parameters (binding affinities, selectivity, stability), potential limitations and future applications.

Keywords: plasmonic; SPR biosensor; viral diagnostics; virus entry inhibitors; drug screening; antiviral agents; SARS-CoV-2; COVID-19



Citation: Mauriz, E.; Lechuga, L.M. Current Trends in SPR Biosensing of SARS-CoV-2 Entry Inhibitors.

Chemosensors **2021**, *9*, 330. <https://doi.org/10.3390/chemosensors9120330>

Academic Editors: Xudong Wang and Hongshang Peng

Received: 31 October 2021

Accepted: 22 November 2021

Published: 25 November 2021

Publisher's Note: MDPI stays neutral with regard to jurisdictional claims in published maps and institutional affiliations.



Copyright: © 2021 by the authors. Licensee MDPI, Basel, Switzerland. This article is an open access article distributed under the terms and conditions of the Creative Commons Attribution (CC BY) license (<https://creativecommons.org/licenses/by/4.0/>).

1. Introduction

Past pandemics of severe acute respiratory syndrome (SARS-CoV-1) in 2003, influenza (H1N1, 1918 and 2009; H2N2, 1958; H3N2, 1968), Middle East respiratory syndrome (MERS) in 2013, and Ebola virus disease in 2014, had previously menaced global health. However, the immense impact of the COVID-19 pandemic outburst in the health condition and socio-economic prospects of the world population has reached unknown proportions [1]. The unexpected risks of recurrent virus outbreaks have stressed the need for searching efficient strategies to prevent viral infections [2]. Generally, antiviral therapeutic interventions rely on the development of candidate drugs following the ‘one bug, one drug’ approach [2,3]. This paradigm is insufficient to lead the fight against viruses due to: (i) the increasing number of emerging viruses; (ii) the presence of undiscovered mammalian virus in the wildlife reservoir; (iii) the lack of broad-spectrum antiviral agents; and (iv) the appearance of drug resistances [4].

Thus, the amelioration of viral infections requires the enlargement of drug candidates with potent antiviral effect and broad-spectrum activities [3]. Novel drug discovery strategies rely on the high throughput screening of different classes of antiviral agents [5]. For example, the increase of antibody drug candidates has provided an efficient approach to treat viral infections due to their specificity [6,7]. However, this selectivity is directed against specific antigens thus limiting their spectrum of activity. To overcome this problem,

the design of antiviral agents has concentrated on the screening of low-molecular-weight fragments that can bind to membrane protein drug targets [5,8]. Fragment-based drug discovery has enabled the identification of a significant number of drugs approved for clinical use [9]. Owing to their low molecular mass, the binding with their target of interest may result in low affinity interactions that require the employment of highly sensitive biophysical techniques for their estimation [8]. Among them, nuclear magnetic resonance (NMR) [10], X-ray crystallography [11], mass spectroscopy [12], isothermal titration calorimetry [13], protein thermal shift [14], affinity capillary electrophoresis [15], weak affinity chromatography [16], have been commonly used to assess protein–drug interactions. More recently, label-free biosensors based on Optical Waveguide Grating (OWG) [17] and reflectometric interference spectroscopy (RIfS) [18] have emerged as valuable tools for evaluating biomolecular interactions [8].

From this perspective, surface plasmon resonance (SPR) biosensors seem to be ideally suited to address this challenge. The application of SPR biosensor technology in the pharmaceutical field has been extensively employed to investigate the binding properties of a broad range of drug candidates from nucleic acids to antibodies [19]. SPR biosensors provide label-free evaluations of molecular interactions between viral targets and their specific recognition element immobilized on the biosensor surface [8,20]. Specifically, SPR sensor devices detect the refraction index variations resulting from the interaction between the analyte and the immobilized bioreceptor occurring on the sensing layer after recognizing the target analyte (Figure 1) [21,22]. The main advantages of SPR biosensor over others biophysical techniques rely on both the short-time response and the capacity to monitor binding activities in real time. SPR analysis offers precise data on the kinetics and thermodynamics of the binding between virus target and the immobilized bioreceptor. SPR sensorgrams provide the association, equilibrium and dissociation phases observed after the injection of the analyte onto the immobilized bioreceptor surface [5,23]. By monitoring binding interactions, SPR biosensors inform on the association (K_a) and dissociation rates (K_d), equilibrium dissociation constants (K_D) and stoichiometry of the interacting biomolecules depending on their binding affinity [6,8,24]. The kinetic information supplied by SPR biosensors is particularly useful for the rapid screening of drug candidates such as virus entry inhibitors. To date, SPR strategies have been successfully applied to the label-free sensitive detection of a wide variety of biomolecules including G-protein coupled receptors, antibodies, aptamers and enzymes [8,24,25].

The role of SPR biosensors in pharmaceutical analysis and viral diagnosis has been previously explored [5,8,19,20,26]. However, the specific utility of SPR biosensors for high-throughput screening of viral inhibitors in the current pandemic context has not been sufficiently addressed [5,6]. Therefore, the aim of this work is to compile recent developments of SPR biosensor approaches in targeting SARS-CoV-2 entry into host cells. This review specifically concentrates on the identification and prioritization of viral inhibitors through the characterization of their binding and kinetic parameters. Current research in SPR antiviral drug development involving fragment-based drug discovery screening of COVID-19 candidate drugs is also reviewed.

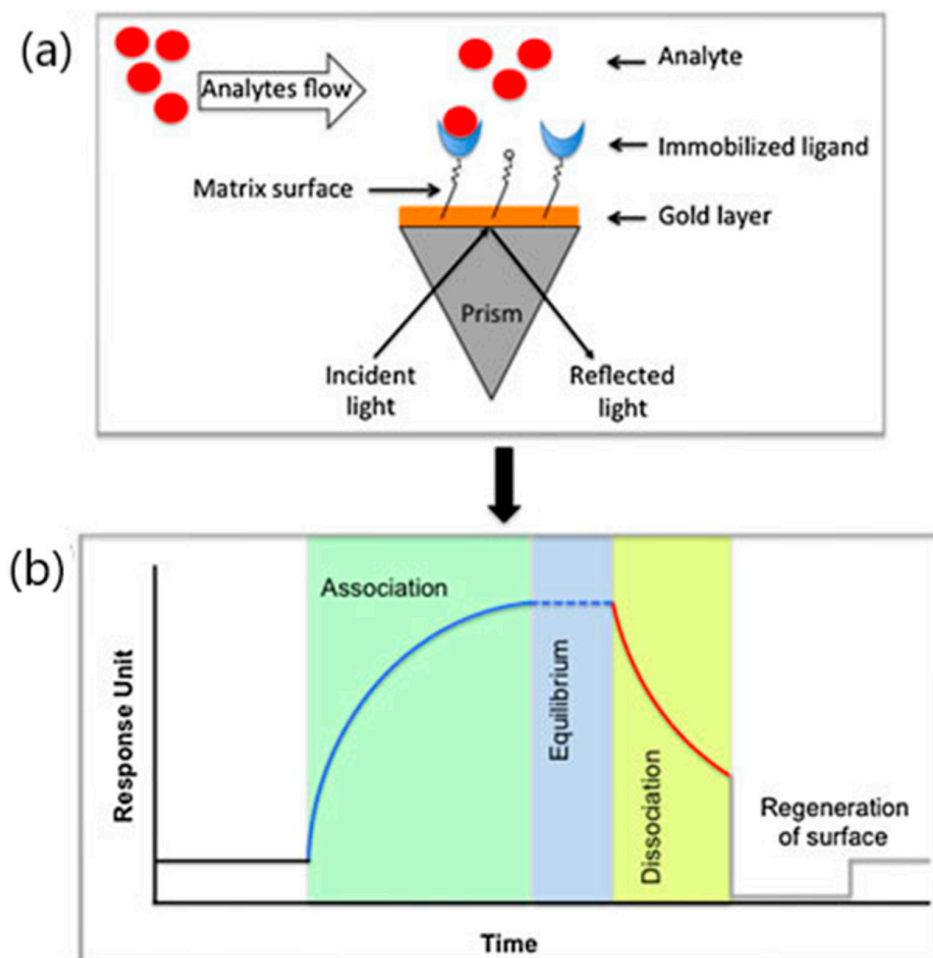


Figure 1. (a) Surface plasmon resonance biosensing configuration. (b) Sensorgram representation of the interaction between the analyte and immobilized biomolecules. Reprinted with permission from Kumar et al. [5] Copyright © 2021 Wiley.

2. Viral Entry and Drug Screening

Viral entry is an indispensable condition to initiate the infection cycle by releasing the viral genome into the infected cell [2,5,27]. The entry process in enveloped viruses involves first the specific binding of the viral surface proteins to the receptors of the cell to be infected and the subsequent viral fusion with the host cell membrane [2,5,27]. Depending on the virus class, the activation of one type or a set of viral envelope glycoproteins, triggers conformational changes in the membrane proteins of both, the virus and the host [4]. A series of intermediate stages comprising pre-fusion, pre-hairpin and post-fusion membrane structural changes complete the viral fusion into the host cell (Figure 2).

Despite the process complexity, the vast majority of viruses present a similar cell entry route regardless of their morphology, genome structure and life cycle. This feature is especially interesting for the design of universal drug strategies that contain viral infections. Tackling viral entry guarantees easier access to the virus target sites while preserving the integrity of the host cell [5]. Particularly, blocking the entry process into host cells seems to be a promising way to protect against viral infection [2]. Among viral entry inhibitors, the most common approaches for inhibiting virus fusion to host cells are based on peptides and small molecules. Although peptide-based inhibitors have been extensively used to block viral fusion, recent strategies have set the focus on the screening of low-molecular-weight compounds known as fragments [8,28].

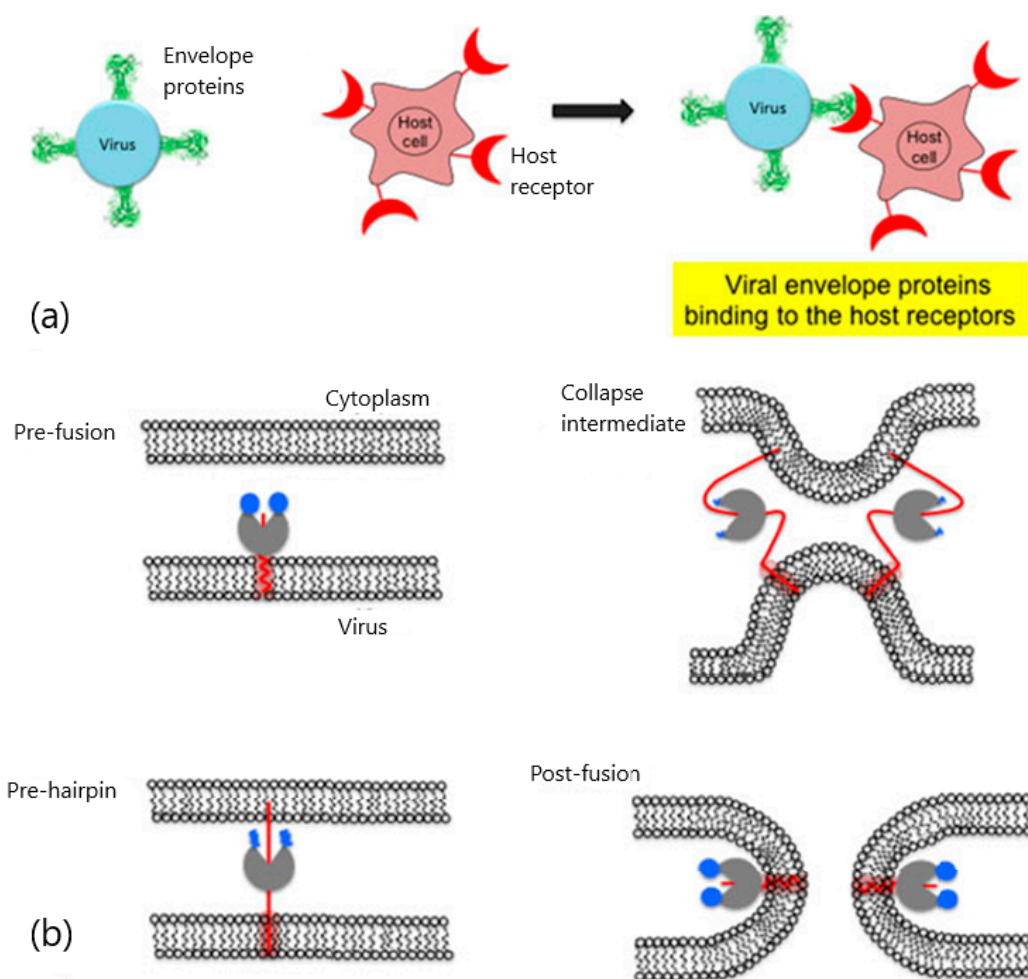


Figure 2. Scheme of viral protein binding to host receptor and membrane fusion mediated by viral proteins (hemagglutinin, HA). (a) Viral surface protein binding to the host cell receptor. (b) Viral protein initiates membrane fusion process with host cell membrane. Reprinted with permission from Kumar et al. [5] Copyright © 2021 Wiley.

Fragment screening has led to the discovery of a considerable number, more than 30 clinical drug candidates in the last 20 years [24]. The utilization of fragment-derived compounds has produced significant benefits in drug discovery since it provides large areas of chemical space [29] and lesser probability of undesired interaction. Additionally, the optimization of the molecular size may lead to improve the affinity and selectivity of the fragments. However, binding between low molecular weight compounds and their ligands often results in low-affinity interactions. Therefore, detection of low fragments requires the employment of highly sensitive biophysical methods (NMR, X-ray crystallography, spectrometry, and so on).

In this context, the SPR biosensor approach has contributed to the characterization and pharmacokinetic profiling of a variety of fragment-based virus inhibitors in the last decade. The role of SPR biosensors is not only limited to complementing other screening techniques but also to informing on the kinetics and binding constants of the low-affinity fragments. Recent advances in SPR biosensor technology have permitted the rapid screening, identification, validation and confirmation of fragments directed against different types of targets (proteases) [30], kinases [29], GPCRs [8] and protein–protein interactions (PPIs) [31]. The following sections describe experimental considerations as well as strengths and limitations in the detection of virus entry inhibitors against SARS-CoV-2.

3. SPR Analysis of SARS-CoV-2 Entry Inhibitors

Coronaviruses (order Nidovirales, family Coronaviridae) are positive-sense single-stranded RNA (ssRNA) with large genomes (27 to 32 Kb in length) coiled inside a helical nucleocapsid. They belong to the subfamily Coronavirinae that includes four genera (alpha (α)-, beta (β)-, gamma (γ)- and delta (δ)-CoVs) [32,33]. Coronaviruses usually contain canonical structural proteins open reading frames (ORF) 1a and 1b, E (envelope protein), M (membrane protein), N (nucleocapsid protein) and S (spike protein) and some accessories proteins such as the membrane-anchored HE (hemagglutinin–esterase) protein expressed by betacoronaviruses [6]. Amongst this genus, SARS-CoV, MERS-CoV and SARS-CoV-2 are considered the most pathogenic human betacoronaviruses. These new coronavirus types are primarily transmitted by aerosols and cause infections of the respiratory tract and atypical pneumonia. Their recurrent break into human populations in 2002–2003 (severe acute respiratory syndrome, SARS-CoV) and 2012 (Middle East respiratory syndrome (MERS-CoV)) has ended with the ongoing global pandemic of coronavirus disease 2019 (COVID-19) caused by SARS-CoV-2 [32]. Coronaviruses enter the infected cell by attaching to cell surface receptors. Particularly, the fusion between the virus and the cell membrane occurs through the binding of the virus S protein and the ACE2 (angiotensin-converting enzyme 2) expressed on the membrane of host cells from the respiratory tract, myocardial tissue, kidney, intestine, male reproductive cells, eyes, vasculature and brain amygdala [34–37](Figure 3). The S protein is not only responsible for giving the virus the appearance of a crown [35] but also in facilitating both the attachment and the entry into the host cells. Specifically, subunit S1 plays an important role in recognizing ACE2 receptors since it contains the N-terminal domain (NTD), the receptor binding domain (RBD) and two conserved subdomains (SD1 and SD2) [6]. On the other hand, subunit S2 mediates the process of membrane fusion. The characterization of the binding affinities between the S1 main domains (NTD and RBD) and the ACE2 human membrane receptor is of primary importance to understand virus infectivity. For example, binding affinities between the RBD of SARS-CoV-2 and human ACE2 are 22 times higher than those of SARS-CoV, thus explaining the stronger infectious capacity of SARS-CoV2. Therefore, inhibiting SARS-CoV-2 entry into host cells seemed to be essential to blocking viral infection [2].

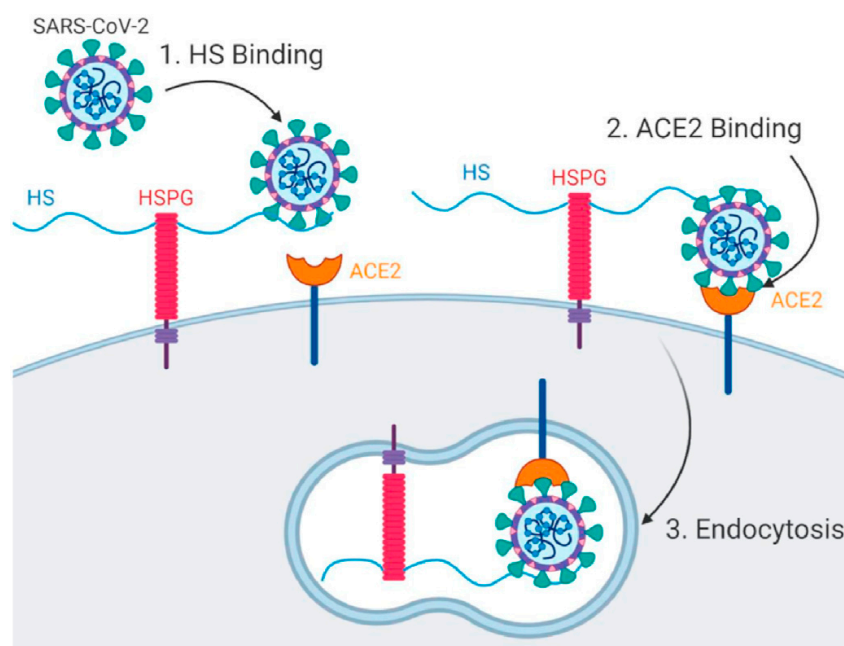


Figure 3. The invasion model of SARS-CoV-2. SARS-CoV-2 first attaches to the cell surface with the aid of heparan sulfate, and then enters the host cell by interacting with ACE2. Reprinted with permission from Wang et al. [6] Copyright © 2021 Elsevier (under CC BY-NC-ND 4.0 license).

3.1. SPR Strategies for Studying the Blocking of ACE2 Receptors

Several SPR approaches have been involved in both pharmaceutical profiling of SARS-CoV-2 entry inhibitors and characterization of the kinetics during the entry process of SARS-CoV-2 into host cells. Most strategies focus on the ability of drug candidates to block ACE2-S-RBD interactions by examining their binding affinities with both ACE2 and RBD proteins. However, a limited number of studies have come forward to assume the detection of affinity constants while screening potential viral inhibitors. Table 1 summarizes the most singular approaches involving either the kinetic analysis or the screening of SARS-CoV-2 inhibitors capable of blocking the ACE2 receptor. The analytical performance characteristics of each method are specifically discussed below.

3.1.1. SPR Biosensor as Primary Screening Method

Zhu et al. [38] investigated protein–protein interactions between human ACE2 and SARS-CoV-2 RBD proteins in search of drug inhibitors. The targeting of surface interactions allowed the discovery of demethylzeylasteral among a library of 960 compounds. First, the binding ability of the proteins was evaluated using ACE2-His as the captured ligand on the SPR sensor chip and S-RBD-mFc as the analyte. To improve the screening efficiency, several models established the contact and dissociation times according to the molecular weights of both the target protein and the screened compound. The screening and affinity analysis of low-molecular-weight compounds was performed following three steps, namely: clean screen, binding level screen and affinity screen. Clean screen permitted the exclusion of 13 compounds more likely to bind residually on the sensor chip surface due to their viscosity. Subsequently, binding level screen enabled the identification of compounds that could bind to the targets of interest and finally, a dose–response curve was assayed to determine their binding affinity. Since residence time was crucial for evaluating the drug efficacy, the association rate constant (k_{on}) and the duration of target occupancy measured by the dissociation rate constant (k_{off}) were examined through a kinetic fitting model. The results confirmed by Isothermal Titration Calorimetry (ITC), showed that demethylzeylasteral could bind to ACE2 and S-RBD with KD values of 1.736 and 1.039 M, respectively. The capacity for blocking ACE2-S-RBD interactions in a dose-dependent manner was also demonstrated by demethylzeylasteral via an SPR-based competitive assay (Figure 4). These results were confirmed by virtual docking, thereby showing that demethylzeylasteral could dock into the ACE2 binding area of S-RBD protein. Therefore, the feasibility of SPR technology as the main method to screen drug inhibitors without the support of traditional screening methods was demonstrated. Moreover, the utility of SPR analysis as a primary screening method has paved the way to acquire information on kinetics and affinity constants more easily by using a single-step format.

Table 1. Key analytical features of SPR biosensor approaches for screening of SARS-CoV-2 inhibitors that block ACE2 receptor classified according to the characteristics of target analyte, analytical approach (namely sensing scheme or biological receptor) and binding affinities (KD equilibrium dissociation constant).

Target Analyte (MW, Common Uses)	Analytical Approach	SPR Instrument	Binding Affinities (KD: Equilibrium Dissociation Constant)	Reference
Demethylzeylasteral (480.59 (g/mol); immunosuppressor, anti-inflammatory, anti-tumoral)	Protein–protein interaction testing Screening and kinetic analysis (binding to ACE2 and S-RBD) Competition assay (blocking RBD-ACE2 interactions)	Biacore T200 (Washington, DC, USA) or S200 instrument (GE Healthcare Life Sciences).	KD = 1.736 mM; k_{on} (1/Ms) = 1989; k_{off} ($\times 10^{-3}$ 1/s) = 3.345 (ACE2) KD = 1.039 mM (S-RBD)	[38]
Sodium lifitegrast (among 21 screened compounds) (637.5 g/mol; keratoconjunctivitis)	SPR screening combined approach Kinetic analysis (binding to S-RBD) Competition assay (blocking RBD-ACE2 interactions)	Biacore S200 system (GE Healthcare Life Sciences)	KD = 1.92 nM (sodium lifitegrast) (KD < 3 mM: rest of compounds) (k_{on} and k_{off} values N/A)	[39]
Thymoquinone (164,201 g/mol; antioxidant, anti-inflammatory, chemotherapeutic)	Binding affinity to ACE2 receptors	Biacore T200 System (GE Healthcare, Uppsala, Sweden)	KD = 32.140 mM (k_{on} and k_{off} values N/A)	[40]
Ginsenoside Ra2, ginsenoside Rb1, ginsenoside Rb3, glycyrrhizic acid and berberine chloride (1211.38, 1109.29, 1079.27, 822.94 and 371.81 g/mol respectively; herbs within clinically effective TCM schemes)	Binding activity of TCM-derived components with SARS-CoV-2 S1 subunit	BIAcore T200 instrument (BIAcore T200, GE Healthcare, Chicago, IL, USA)	KD = 55.6 mM (ginsenoside Ra2); KD = 29.7 mM (ginsenoside Rb3); KD = 2.0 mM (ginsenoside Rb1); KD = 66.8 mM (glycyrrhizic acid); KD = 23.9 mM (berberine chloride) (k_{on} and k_{off} values N/A)	[41]
Quinoline-2-carboxylic acids (3 compounds) (173.168 g/mol, <i>Ephedra sinica</i> extracts; lung diseases treatment)	Binding affinity constants (to S-RBD) Competition assay (blocking RBD-ACE2 interactions)	BIAcore T200 instrument (GE Healthcare Life Sciences)	KD = 0.60–5.37 mM (k_{on} and k_{off} values N/A)	[42]
<i>Radix Scutellariae</i> extract: Oroxylin A (284.26 g/mol; respiratory diseases, diabetes, diarrhea treatment)	Binding affinity constants (to ACE2)	Open SPR™ (Nicoya Lifesciences, Waterloo, Canada)	KD = 9.72×10^{-6} M (k_{on} and k_{off} values N/A)	[43]
Polyphenols: corilagin and TGG (636.46 and 423.40 g/mol, respectively; antioxidant, anti-inflammatory, and antidiabetic treatments)	Binding affinity constants (to S-RBD) Binding affinity of TGG and corilagin with RBD mutations of three main SARS-CoV-2 variants Competition assay (blocking RBD-ACE2 interactions)	Biacore T200 instrument (GE Healthcare)	KD = 1.8 nM (corilagin) KD = 1.3 nM (TGG) (k_{on} and k_{off} values N/A)	[44]

Table 1. Cont.

Target Analyte (MW, Common Uses)	Analytical Approach	SPR Instrument	Binding Affinities (KD: Equilibrium Dissociation Constant)	Reference
Erythrodiol (442.7 g/mol; <i>Momordica charantia</i> component: treatment of nephropathy, neuropathy, gastroparesis, cataracts and atherosclerosis)	Binding affinity constants (to SARS-CoV-2 S1 subunit)	Open SPR instrument (Nicoya Lifescience, ON, Canada)	KD = 1.15 μ M (k_{on} and k_{off} values N/A)	[45]
Histamine H1 receptor antagonists: doxepin, chlorpheniramine, and doxylamine (279.376, 274.788 and 270.369 g/mol respectively; allergic rhinitis, allergic conjunctivitis and allergic dermatitis)	Analysis of bimolecular interactions with ACE2 receptor	Open SPR TM (Nicoya, Waterloo, Canada)	KD = 9.54 mM (doxepin); KD = 0.30 mM (chlorpheniramine); KD = 47.3 mM (doxylamine) (k_{on} and k_{off} values N/A)	[46]
Azelastine (381,898 g/mol; allergic conjunctivitis)	Kinetic analysis (binding to ACE2 receptor)	Open SPR TM (Nicoya, Waterloo, Canada)	KD = 0.258 μ M (k_{on} and k_{off} values N/A)	[47]
Desloratadine and loratadine (310.82 and 382.88 g/mol; treatment of allergic disease)	Kinetic analysis (binding to ACE2 receptor)	Open SPR TM (Nicoya, Waterloo, Canada)	KD = 9.13 μ M (desloratadine); KD = 0.1.02 μ M (loratadine) (k_{on} and k_{off} values N/A)	[48]
Chloroquine (CQ) and hydroxychloroquine (HCQ) (319.872 and 335.872 g/mol; antimalarial drugs)	Kinetic analysis (binding to ACE2 receptor)	Open SPR TM (Nicoya, Waterloo, Canada)	KD = $(7.31 \pm 0.62) \times 10^{-7}$ M (CQ) KD = $(4.82 \pm 0.87) \times 10^{-7}$ M (HCQ) (k_{on} and k_{off} values N/A)	[49]
Trifluoperazine (Tri); thioridazine (Thi); chlorpromazine (Chl), aripiprazole (Ari), tiapride (Tia) (407.497, 370.6, 318.86, 448.385 and 328,427 g/mol, respectively; antipsychotic drugs)	Kinetic analysis (binding to ACE2 receptor)	Open SPR TM (Nicoya, Waterloo, Canada)	KD = $(7.03 \pm 3.28) \times 10^{-6}$ M (Tri); KD = $(8.91 \pm 5.25) \times 10^{-5}$ M (Thi); KD = $(1.38 \pm 0.38) \times 10^{-5}$ M (Chl); KD = $(7.88 \pm 0.49) \times 10^{-6}$ M (Ari), and $(3.33 \pm 3.13) \times 10^{-5}$ M (Tia) (k_{on} and k_{off} values N/A)	[50]

MW: Molecular weight; k_{on} = association rate; k_{off} = dissociation rate; KD = equilibrium dissociation constants; N/A = not available; TCM: traditional Chinese medicine.

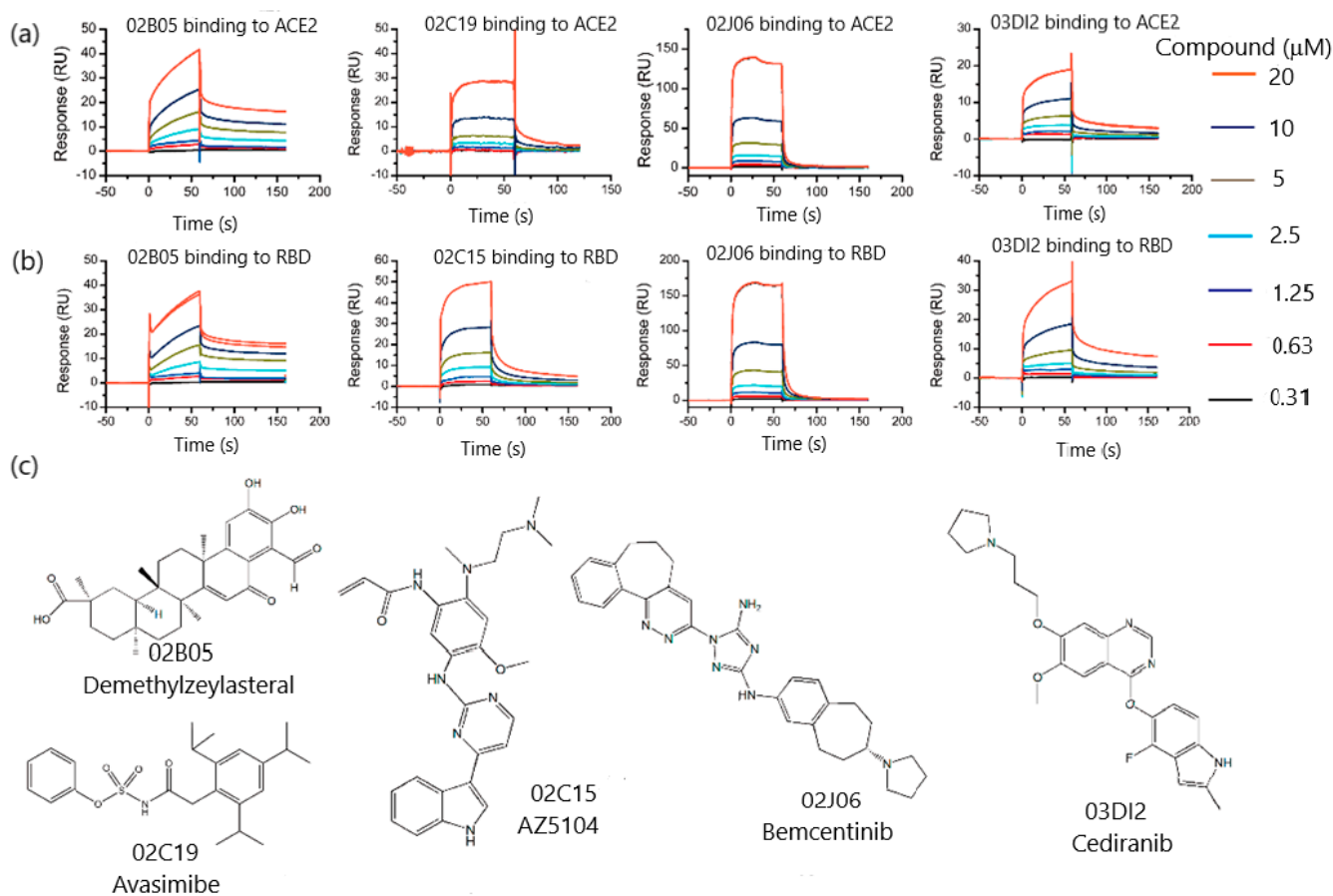


Figure 4. (a) Sensorgrams of compounds identified from the affinity screening bound to ACE2; (b) sensorgrams of compounds identified from the affinity screening bound to S-RBD. (c) Chemical structures of compounds discovered during SPR affinity screening. Reprinted with permission from Zhu et al. [38]. Copyright © 2021 MDPI.

Following the same trend, a multidisciplinary approach took advantage of a dual strategy involving both molecular docking and SPR combined screens [39]. Day et al. reported a blended procedure comprising molecular modeling and SPR interrogation to identify potential blocking candidates of RBD SARS-CoV-2–ACE2 interactions, from two libraries of 57,641 and 3141 compounds, respectively. Primarily, the role of SPR biosensing in these experiments consisted of the initial screening of compounds that bound ACE2, followed by the analysis of binding affinities of either the compounds identified by molecular docking or SPR. Measured affinities were in agreement with those predicted by molecular docking. The combination of both screening techniques allowed the characterization of the binding affinities of 17 compounds for ACE2 and 6 for SARS-CoV-2 RBD that showed <3 mM affinity to their respective protein targets. An SPR-based competition assay was also implemented to examine the ability of 12 ACE2 and 6 RBD binders for blocking RBD–ACE2 interactions. By using immobilized ACE2, SPR analysis demonstrated the ability of 11 of the 12 compounds to inhibit the interaction between a RBD mimic-peptide and recombinant human ACE2. Among them, two compounds, Evans blue and Irinotecan, could block completely the RBD–mimic peptide–ACE2 interaction. Virus-like particles (VLP) expressing SARS-CoV-2 spike protein were also immobilized in the SPR sensor chips to study the blockade of human ACE2–VLP spike protein interactions. Using this immobilization format one compound, sodium lifitegrast, demonstrated the elimination of 99.8% of the RBD–ACE2 interaction. Finally, 11 compounds were selected to prove their antiviral potency against SARS-CoV-2 infection of Vero-E6 cells. These

experiments demonstrated that three compounds (Evans blue, lifitegras and lumacaftor) could block SARS-CoV-2 activity and exhibited dose-dependent antiviral in vitro potency without showing cytotoxicity. In this work, SPR biosensing proved its practical functionality not only to repurpose and identify potential drugs as SARS-CoV-2 entry inhibitors but also to design chemical scaffolds for drug development.

3.1.2. Kinetic Analysis of Natural Products Obtained from Plants

Despite these advances, the number of studies that report combined screens of molecular docking and SPR is still scarce. Most of the strategies make use of SPR studies to determine binding affinities between drug candidates and protein receptors. Several works have focused on the characterization of SARS-CoV2 potential inhibitors by examining the affinity with their target proteins. In this sense, the discovery of new inhibitors from the repurposing of commercial medicines has played a significant role. For instance, Xu et al. confirmed the binding of thymoquinone, a phytochemical compound obtained from the plant *Nigella sativa* to ACE2 receptor [40]. SPR analysis revealed the capacity of thymoquinone as a potential drug candidate to block ACE2 receptor. By flowing thymoquinone over the sensor surface immobilized with ACE2 protein, thymoquinone–ACE2 interactions showed a strong dependence on the dosage with an equilibrium dissociation constant (KD) of 32.140 mM. These results suggest that thymoquinone may block the virus entry into the host cell by interfering the S1-ACE2 binding. This assumption was confirmed by half maximal inhibitory concentration (IC50) and half maximal cytotoxic concentration (CC50) values for SARS-CoV-2 pseudovirus. However, the specificity of the assays should be further studied because of the pan-assay interference properties of thymoquinone.

The search for spike protein inhibitors among bioactive compounds of traditional Chinese medicine (TCM) has also been explored [41]. SPR analysis was applied to the determination of the binding activity of 66 TCM-derived components with SARS-CoV-2 S1 subunit. From the 66 components selected by molecular docking virtual screening, 19 were excluded due to their insolubility in the assay buffer (HBS-EP+). The binding activity of the remaining 44 compounds was verified using S1 subunits of SARS-CoV-2, MERS-CoV and SARS-CoV as immobilized receptors. The characterization of the binding activities demonstrated that five compounds: ginsenoside Ra2 (ZZY-8), ginsenoside Rb1 (ZZY-9), ginsenoside Rb3 (ZZY-13), glycyrrhizic acid (ZZY-44) and berberine chloride (ZZY-54) showed high affinity for the SARS-CoV-2 S1 subunit, being concentration-dependent, with KD values between 0.47 and 9.44 mM. Similar binding activity was found with S1 subunits of MERS-CoV while those obtained for SARS-CoV were reduced. The high affinities of these five active compounds with the binding interface of SARS-CoV-2 S1 could be exploited to block the interaction between the S protein and human ACE2 protein. The five compounds discovered by SPR were further investigated to determine their activity in the interaction between the RBD of SARS-CoV-2 and ACE2, by a NanoBit assay. The results showed that glycyrrhizic acid (ZZY-44) was the best candidate to disrupt the interaction between the RBD of SARS-CoV-2 and ACE2, exhibiting no toxicity at high concentrations. Although SPR analysis did not contribute to the primary screening of TCM compounds, the characterization of the binding activities with S1 subunits of SARS-CoV-2, led to the discovery of glycyrrhizic acid as a potential nontoxic broad-spectrum anti-coronavirus multitarget inhibitor.

Mei et al. followed a similar approach for discovering active compounds in *Ephedra sinica*, a broadly used medicinal plant in traditional Chinese medicine [42]. Particularly, it was investigated with regards to its capacity to disrupt the interaction between ACE2 and the SARS-CoV-2 spike protein RBD. First, SPR biosensing was used to validate the inhibition activity of SARS-CoV-2 RBD/ACE2 interaction. By immobilizing RBD on the sensor chip, ACE2 could bind to RBD in a dose-dependent manner with an affinity of 20.19 nM. Similarly, the kinetics and binding activity of the compounds previously identified by HPLC-Q-TOF-MS/MS and NMR were also evaluated. Finally, SPR competition inhibition assays were performed to explore the inhibitory effect of the selected compounds (Figure 5).

The interference of these compounds with the binding interface of SARS-CoV-2 RBD was demonstrated by flowing the RBD–compound mixture over immobilized ACE2. The results showed that three compounds (quinoline-2-carboxylic acids) could block the ACE2–RBD interaction, thus suggesting their potential to inhibit SARS-CoV-2 virus infection. The inhibitory efficacy on ACE2–RBD interaction of these quinoline-2-carboxylic acids was verified by molecular docking. This work exemplifies the contribution of SPR technology in supporting other techniques to discover potential therapeutic compounds in the treatment of COVID-19.

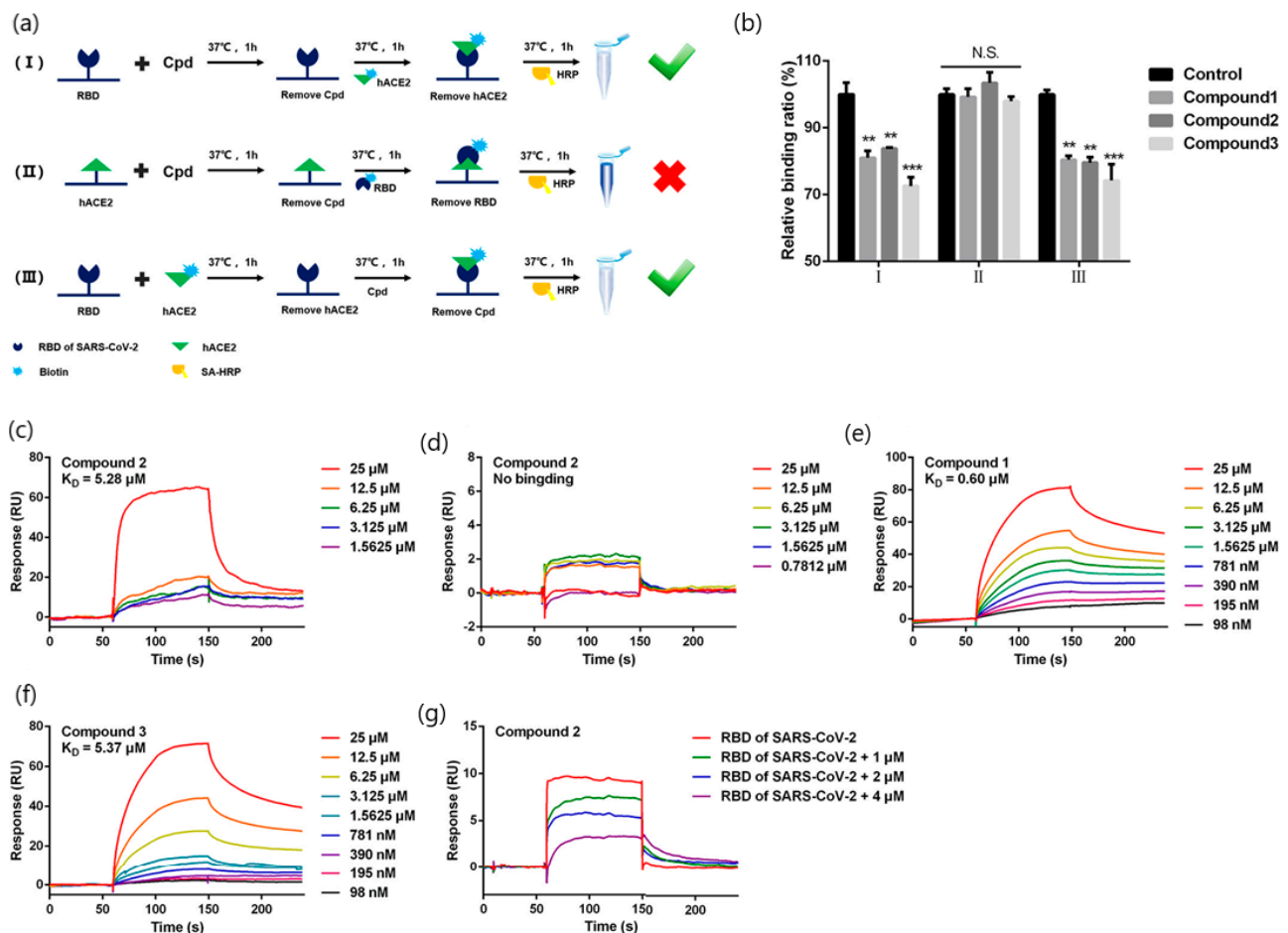


Figure 5. Quinoline-2-carboxylic acids inhibited ACE2–RBD interaction by directly binding to SARS-CoV-2 RBD. (a) The time-of-addition experimental scheme. (b) The relative binding amount under different conditions. Compound 2 were injected in two-fold serial dilutions over SARS-CoV-2 RBD (c) or ACE2 (d) immobilized on the biosensor chip. Compound 1 (e) or 3 (f) were injected in two-fold serial dilutions over SARS-CoV-2 RBD immobilized on the biosensor chip. (g) Various amounts of compound 2 were incubated with 22.5 nM SARS-CoV-2 RBD at 37 °C for 1 h, then each mixture was injected over ACE2 immobilized on the biosensor chip. TCM-derived components. Reprinted with permission from Mei et al. [41]. Copyright © 2021 Elsevier.

Gao et al. reported the combined use of molecular docking and SPR analysis for evaluating the binding properties of oroxylin A (another TCM-derived compound) with ACE2 protein [43]. CMC method was used as a screening method to isolate oroxylin A from *Radix Scutellariae* extract. After proving the anti-viropepexis effect of the screened compound in HEK293T cells expressing ACE2 receptors, SPR assays confirmed that oroxylin A could bind to ACE2 ($K_D = 9.72 \times 10^{-6} \text{ M}$), thereby paving the way to further investigation on the antiviral properties of this plant extract.

Polyphenols have also been considered as potential antiviral drug candidates for inhibiting SARS-CoV2 infection. The therapeutic potential of polyphenols obtained from

plants have been investigated by molecular docking and molecular dynamics (MD) simulations. Several natural compounds which can block the interaction with ACE2 have been recently identified. Among them, the interaction of corilagin (C₂₇H₂₂O₁₈) and 1,3,6-tri-Ogalloy-b-D-glucose (TGG) (C₂₇H₂₄O₁₈) with Spike protein/ACE2 interface have been examined by numerical methods to further evaluate their binding affinities with SPR and ELISA [44]. SPR experiments indicated that both polyphenols could bind to the immobilized RBD, showing equilibrium dissociation constants in the nanomolar range, 1.8 nM for corilagin/RBD and 1.3 nM for TGG/RBD, respectively. On the other hand, a significant binding to ACE2 was not observed of either corilagin, or TGG in the 1 to 80 nM range (Figure 6). The interactions between ACE2 and RBD were also explored, displaying KD values of 41 nM (ACE2 to immobilized RBD) and 63 nM (RBD to immobilized ACE2), as corroborated by other studies. Finally, the ability of these compounds to prevent RBD/ACE2 interactions were evaluated flowing TGG/corilagin mixtures previously incubated with RBD over ACE2 immobilized sensor chips. SPR assays demonstrated that both TGG (12.5 nM) and corilagin (50 nM) could inhibit RBD/ACE2 binding. Furthermore, the binding affinity of TGG and corilagin with RBD mutations of three main SARS-CoV-2 variants (E484K, N501Y and E484K/N501Y) was determined using MD simulations. Overall, the numerical approach suggested that the RBD residues remain accessible at the interface with ACE2 despite these mutations. Although SPR experiments only served to validate the numerical protocol, these results show that corilagin did not interfere with the recognition of ACE2 by RBD for the structures with the N501Y mutant while TGG was more effective in these mutants. Therefore, further investigation is needed to monitor the selectivity of these compounds with regards to other virus-binding sites and their in vivo behavior.

The interest in natural remedies has led to the investigation of the antiviral properties of other compounds obtained from vegetables. For instance, erythrodiol, an extract component of *Momordica charantia*, commonly known as bitter melon, was identified by molecular docking to study their capacity to inhibit SARS-CoV-2 infections [45]. In this work, SPR biosensor was used to examine the interaction of erythrodiol and S1 and S2 domains of the SARS-CoV-2 spike protein. SPR results revealed that erythrodiol has a strong binding affinity (equilibrium dissociation constant, KD = 1.15 μM) with S2, the active site of the SARS-CoV-2 spike protein. Therefore, the combination of docking, ADME (absorption, distribution, metabolism and excretion) properties, and SPR contributed to confirm the inhibition activity of erythrodiol to block the binding of the spike protein.

3.1.3. SPR Role in Drug Repurposing

Other interesting approaches have made use of SPR biosensing for drug repurposing of histamine H1 receptor antagonists [46,47]. Antihistamine drugs are commonly used to treat allergic diseases by downregulating allergic inflammation. However, several studies have recently described their effect as inhibitors of Ebola, Marburg [51], and influenza viruses [52] into host cells. By following this hypothesis, Ge et al. proved the antiviral properties of histamine H1 receptor antagonists through the evaluation of their binding affinities with ACE2 receptor. On that premise, a series of histamine H1 receptor antagonists with ACE2 binding activity were screened by cell membrane chromatography (CMC). SPR assays were performed to detect biomolecular interactions of the ACE2 protein immobilized on the sensor chip and three compounds (doxepin, chlorpheniramine, doxylamine) identified by CMC. The calculation of the kinetic values showed equilibrium dissociation constants (KD) of 9.54 ± 0.30 , 10.5 ± 2.1 and 47.3 ± 5.2 μM for doxepin, chlorpheniramine and doxylamine, respectively. The smallest value was obtained for doxepin, being in accordance with the activity showed for inhibiting pseudovirus entry. SPR measurements were further confirmed by analyzing the docking conformation of doxepin with ACE2, demonstrating that the binding to the S protein prevented the binding with ACE2 protein leading to the subsequent inhibition of the virus entry. A similar concept was applied by the same authors for monitoring the binding of azelastine, another antihistamine, to ACE2. Direct binding of azelastine to immobilized ACE2 showed Kd

values of 0.258 ± 0.48 mM, exhibiting a stronger inhibitory effect at low concentrations. Therefore, SPR analysis contributed to the discovery of dual-target clinical drugs that can inhibit virus entry while reducing the inflammatory response evoked by COVID-19.

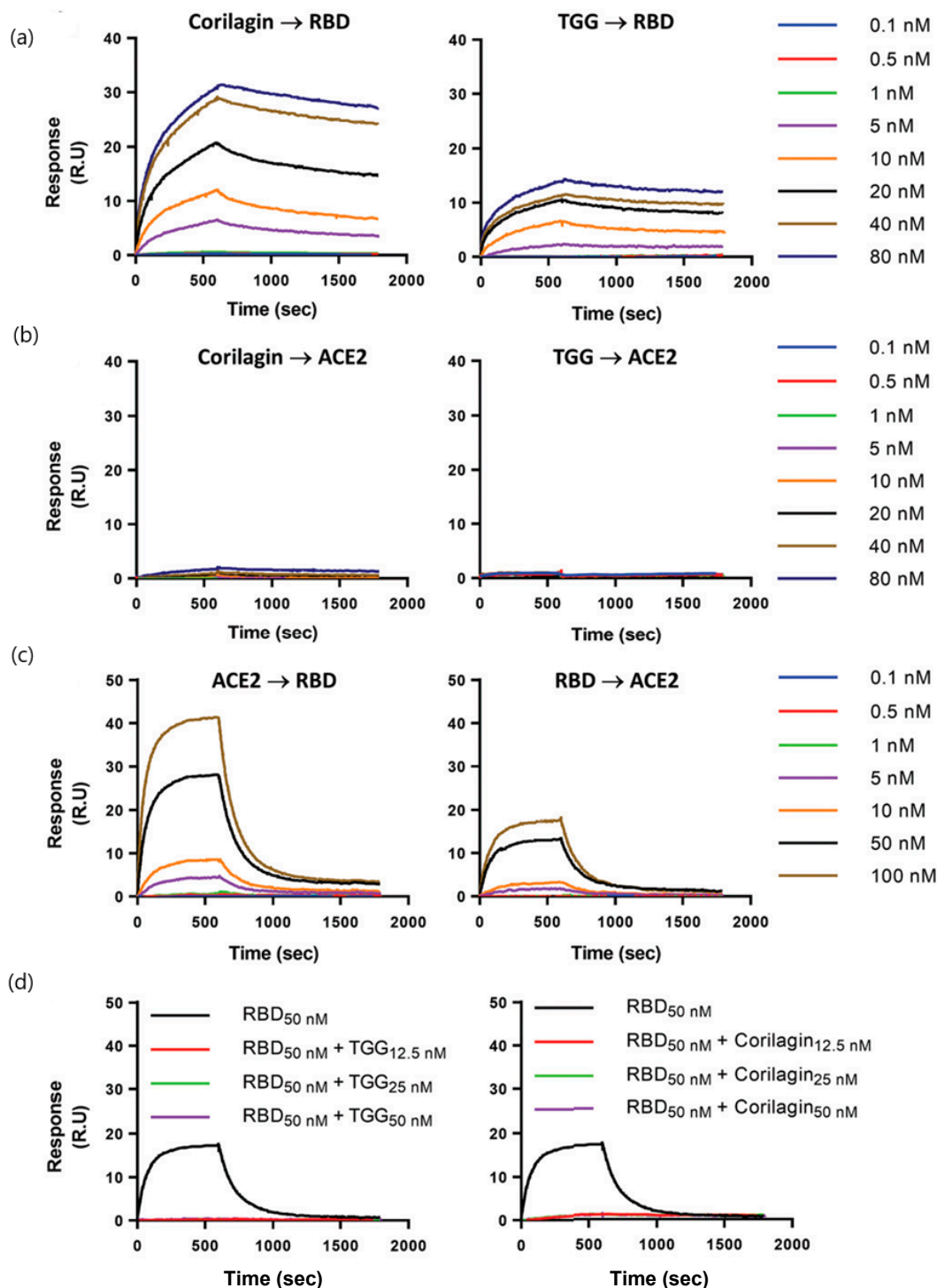


Figure 6. Characterization of molecular interactions by surface plasmon resonance. (A and B) Binding kinetics of corilagin and TGG on immobilized (a) RBD and (b) ACE2. The recombinant proteins RBD and ACE2 are respectively immobilized on a CM5 sensor chip and increasing concentrations of polyphenols are injected to evaluate binding kinetics. (c) Kinetics of ACE2 binding to immobilized RBD (left panel) and kinetics of RBD binding to immobilized ACE2 (right panel). (d) Pre-incubation of RBD (50 nM) for 30 min with increasing concentrations of corilagin or TGG inhibit the binding of RBD to immobilized ACE2. Reprinted with permission from Binette et al. [44] Copyright © 2021 Royal Chemical Society.

In this framework, the antiviral effect of histamine H1 antagonist approved drugs loratadine (LOR) and desloratadine (DES) has also been investigated. A combined approach involving cell membrane chromatography and SPR sensing was developed to determine the binding affinity of loratadine and desloratadine to ACE2 receptor [48]. On the one hand, CMC showed that the specific binding durations of LOR and DES to ACE2 receptor were 2.49 and 51.8 min, respectively, showing that desloratadine could bind to ACE2 receptor more strongly than loratadine. These findings were confirmed by SPR assays where desloratadine exhibited higher binding constants ($K_D = 9.13 \pm 0.67 \times 10^{-6}$ M) than loratadine ($1.02 \pm 0.38 \times 10^{-7}$ M). Similarly, molecular docking determinations proved that desloratadine could bind to ACE2 through one hydrogen bond with LYS31 while loratadine did not form hydrogen bonds, thus validating the SPR results. Since the blocking effect was only measured on the entry of SARS-CoV-2 spike pseudotyped virus into ACE2h cells, the efficacy of loratadine and desloratadine may need further evaluation in native viruses and animal models.

Chloroquine (CQ) and hydroxychloroquine (HCQ) are well-known compounds for their antimalarial properties. However, their use as anti-COVID drugs remains controversial due to the risk of cardiotoxicity reported in some clinical trials [53]. At the same time, other studies suggested that CQ and HCQ could disrupt ACE2 terminal glycosylation thus preventing the binding with viral S protein. The ability to block ACE2 binding and inhibit virus entry into host cells has been explored by using an SPR approach [49]. Wang et al. performed SPR assays to assess the binding activity of CH and HCQ with ACE protein immobilized on the sensor chips. SPR studies confirmed virtual molecular docking tests, showing binding constants K_D of $(7.31 \pm 0.62) \times 10^{-7}$ M and $(4.82 \pm 0.87) \times 10^{-7}$ M, for CQ and HCQ, respectively. These results demonstrated that CQ and HCQ could bind to ACE2 protein. Despite these findings, the unwanted effects caused by CQ and HCQ together with the inefficiency to reduce deaths from COVID-19 suggest that the role of CQ and HCQ as inhibitory drugs in suppressing the entrance of the SARS-CoV-2 virus while blocking infection of human cells will need further confirmation.

The search for new uses of already existing drugs has led to the investigation of the antiviral properties of antipsychotic drugs [50]. Previous studies have suggested that antipsychotic drugs can inhibit replication of SARS-CoV or MERSCoV viruses, Hepatitis B Virus (HBV), measles virus germination, and HIV infection [54]. On the other hand, preclinical studies have reported that psychotropic medical treatments can protect from severe forms of COVID-19. Based on these considerations, Lu et al. examined the affinity for ACE2 of five antipsychotic drugs previously screened by cell membrane chromatography. The binding of these compounds (trifluoperazine (Tri); thioridazine (Thi); Chlorpromazine (Chl), aripiprazole (Ari), tiapride (Tia)) with ACE2 protein, showed high affinity as demonstrated by their K_D values: $(7.03 \pm 3.28) \times 10^{-6}$ M, $(8.91 \pm 5.25) \times 10^{-5}$ M, $(1.38 \pm 0.38) \times 10^{-5}$ M, $(7.88 \pm 0.49) \times 10^{-6}$ M and $(3.33 \pm 3.13) \times 10^{-5}$ M, respectively (Figure 7). SPR studies were complemented with molecular docking to identify modified regions. This work suggested that antipsychotic drugs with phenothiazine scaffolds had potential antiviral ability. However, they were not completely effective for preventing cell invasion, since these antipsychotic drugs bind to different amino acids, thereby blocking small areas of SARSCoV-2 binding to ACE2. As a result, the use of combined cocktails of these drugs could contribute to preventing virus infections.

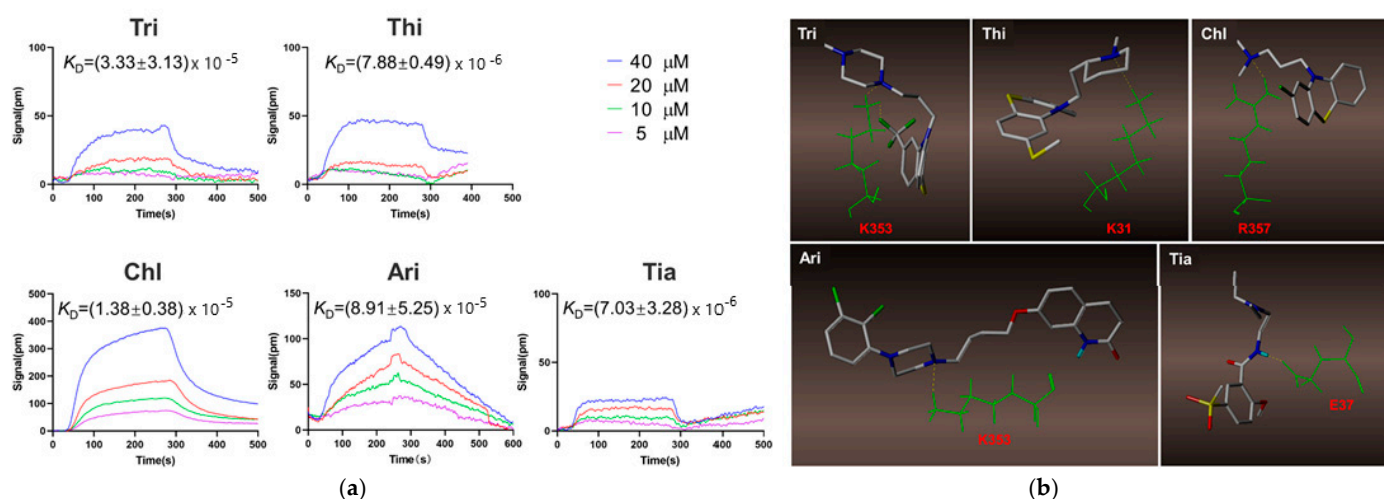


Figure 7. Study of the binding activity of five antipsychotic drugs: trifluoperazine (Tri); thioridazine (Thi); chlorpromazine (Chl), aripiprazole (Ari), tiapride (Tia). (a) The SPR analysis of the five antipsychotic drugs. (b) The virtual molecular docking analysis of the five APDs. Reprinted with permission from Lu et al. [50]. Copyright © 2021 Elsevier.

3.1.4. SPR Biosensors as Diagnostic Tools to Detect Neutralizing Antibodies

Alternatively, SPR biosensing has been tested as a diagnostic method to validate the results obtained by enzyme-linked immunosorbent assay (ELISA) for detecting receptor-binding antibodies in sera. SPR serological assays were conducted to demonstrate antibody binding to the SARS-CoV-2 spike protein while blocking the ACE2 receptor [55]. Specifically, the role of SPR biosensing consisted of the assessment of serological responses of different antibodies' epitopes when competing with ACE2 or blocking the binding to SARS-CoV-2. Therefore, by evaluating the neutralizing activity of antibodies, SPR assays proved their utility to target viral surface proteins and inhibit SARS-CoV-2 spike interaction with its receptor. The binding of scFv, Fab, and IgG (immunoglobulin G) of CR3022 antibodies to the RBD of SARS-CoV-2 has also been investigated by SPR in a silkworm-baculovirus expression system [56]. SPR analysis demonstrated that the IgG antibodies produced by silkworms had almost the same affinity to S protein that those produced in mammalian expression system. This is another singular approach in which an SPR sensor can contribute to determine antibody responses when examining vaccine candidates against SARS-CoV-2 viral spike protein [57]. On the one hand, SPR measurements confirmed that rabbit sera contained anti-spike antibodies: 80% IgG, 15% IgA (immunoglobulin A) antibodies and minimal IgM (immunoglobulin M). At the same time, the generation of antibodies by the three antigens (S1 + S2 ectodomain, S1 domain and RBD) was also investigated. The kinetic analysis performed by SPR revealed that all three domains, except for the S2, induced the fabrication of neutralizing antibodies against SARS-CoV-2 (Figure 8). In the same way, Ye et al. made use of SPR biosensing technology to characterize the binding affinity between single-domain antibodies (i.e., nanobody), Nanosota-1 and SARS-CoV-2 RBD, using recombinant ACE2 as a comparison [58]. Nanobodies were identified by screening a camelid nanobody phage display library. The greater ability to block ACE2 receptor was demonstrated by the drug candidate that possessed an Fc tag (Nanosota-1C-Fc), showing a KD value 15.7 pM with RBD. This finding suggested that the binding affinity was ~3000 times tighter when compared to the RBD-binding affinity of ACE2. Additionally, the association rates indicated faster binding to the RBD than ACE2, as well as slower dissociation rates. As a result, it was proved that Nanosota-1C-Fc could inhibit SARS-CoV-2 pseudovirus ~160 times more efficiently than ACE2. The efficacy as preventing and therapeutic agent against live SARS-CoV-2 infection was confirmed by hamster and mouse models. Therefore, SPR biosensing demonstrated its functionality in monitoring the immune response generated by the different antigens of the spike proteins after vaccination against SARS or SARS-CoV-2 infection.

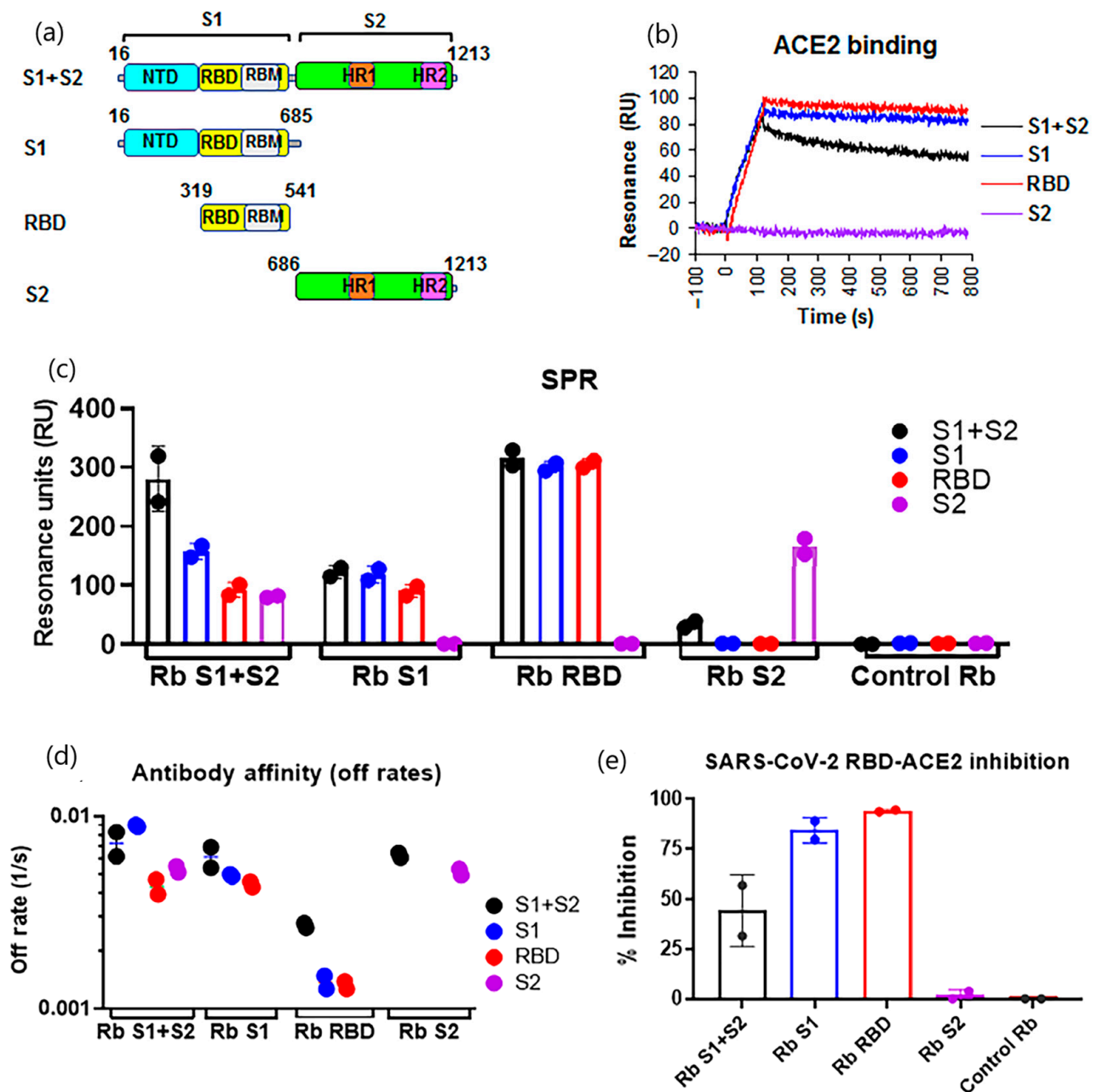


Figure 8. SARS-CoV-2 spike binding and SARS-CoV-2 neutralization by serum antibodies generated after rabbit immunization with spike antigens. (a) Schematic representation of the SARS-CoV-2 spike protein and subdomains. Spike S1 + S2 ectodomain (amino acids 16 to 1213), S1 domain (amino acids 16 to 685), receptor binding domain (RBD) (amino acids 319 to 541) and S2 domain (amino acids 686 to 1213). (b) Binding of purified proteins to human ACE2 (hACE2) proteins in SPR. Sensorgrams represent binding of purified spike proteins on low-density His-captured chips to hACE2 protein (5 μ g/mL). (c) SPR binding of antibodies from two rabbits each immunized twice with SARS-CoV-2 antigens to spike protein and domains from SARS-CoV-2 (S1 + S2, black; S1, blue; RBD, red; and S2, purple). Total antibody binding is represented in maximum resonance units (RU) in this figure for 10-fold serum dilution. (d) Antibody off-rate constants were directly determined from the serum sample interaction with SARS-CoV-2 spike ectodomain (S1 + S2), S1, S2, and RBD using SPR in the dissociation phase. (e) RBD-hACE2 competition assay. Percent inhibition of hACE2 binding to RBD in the presence of 1:50 dilutions of post-second. Reprinted with permission from Ravichandran et al. [57]. Copyright © 2020 AMER ASSOC ADVANCEMENT SCIENCE (Distributed under a Creative Commons Attribution License 4.0 (CC BY)).

3.2. SPR Strategies for the Development of SARS-CoV-2 Main Protease Inhibitors

Although most of the SPR approaches rely on the monitoring of binding affinities between the RBD of the spike S protein and ACE2 receptors, SARS-CoV-2 possesses 16 nonstructural proteins. Among them, the main protease (Mpro), also known as 3-chymotrypsin-like protease (3CLpro) or chymotrypsin-like protease, is an essential enzyme that plays an important role in mediating the virus replication and processes the polyproteins that are translated from CoV RNA [59–61]. Mpro consists of three domains (I to III), with the active site located between domains I and II (3CLpro) (Figure 9) [59,60]. Owing to the importance of 3CLpro on the life cycle of the virus, the development of Mpro inhibitors could be a promising strategy to block viral replication and prevent virus infection. In addition, the main protease is highly conserved in coronavirus and has no closely related homologue in humans with a similar cleavage specificity, and then 3CLpro has become an attractive target for the design of broad antiviral drugs (Table 2).

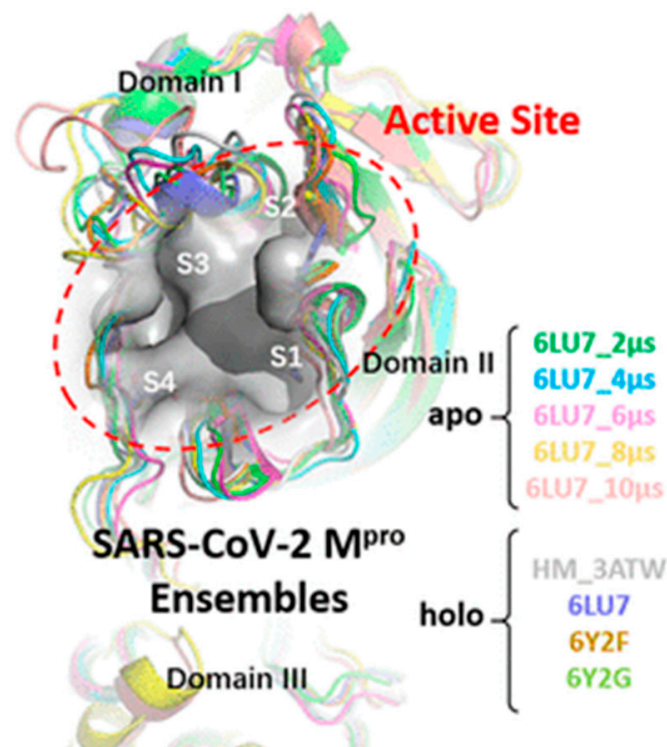


Figure 9. Ensemble SARS-CoV-2 Mpro 3D structures shown in cartoon representation with different colors. Domain I (residues 10 to 99), Domain II (residues 100 to 182) and Domain III (residues 198 to 303) of the protease are labeled. The substrate-binding site (active site) of Mpro composed of four subsites (S1, S2, S3, and S4) marked by the gray surface. Reprinted with permission from Yang et al. [62]. Copyright © 2021 Elsevier.

Table 2. Key analytical features of SPR approaches for screening of SARS-CoV-2 inhibitors that bind to Mpro classified according to the characteristics of target analyte, analytical approach (namely, sensing scheme or biological receptor) and binding affinities (KD equilibrium dissociation constant).

Target Analyte (MW; Common Uses)	Analytical Approach	SPR Instrument	Binding Affinities (KD = Equilibrium Dissociation Constant)	Reference
Quercetin, Luteolin, kaempferol, naringenin and epigallocatechin-3-gallate (302.236, 286.24, 286.23, 272.257 and 458,372 g/mol, respectively; antioxidant, anti-inflammatory)	Kinetic analysis (binding to 3CLpro)	Open SPR instrument (Nicoya Life Science, Inc., Kitchener, Canada)	KD = 1.24 μ M; KD = 1.63 μ M (luteolin); KD = 1.70 μ M (kaempferol); KD = 2.87 μ M (naringenin); KD = 6.17 μ M (epigallocatechin-3-gallate). (k_{on} and k_{off} values N/A)	[63]
Punicalagin: PA; ellagic acid: EA; tannic acid: TA, pentagalloyl glucose: PGG; ginnalin A, and gallic acid: GA; urolithins: UB and pyrogallol: PYG (1.084.71, 302.297, 1701.19, 940.67, 468.4, 170.12, 212.20 and 126.11 g/mol respectively; antioxidant, anti-inflammatory)	Kinetic analysis and binding affinities (binding to 3CLpro)	Biacore T200 instrument (GE Healthcare; Marlborough, MA, USA)	KD = 6.8×10^{-6} M; k_{on} (1/Ms) = 697.3; k_{off} (1/s) = 0.0047 (PA) KD = 2.7×10^{-6} M; k_{on} (1/Ms) = 4755.2; k_{off} (1/s) = 0.0130 (EA); KD = 1.13×10^{-6} M; k_{on} (1/Ms) = 6309.0; k_{off} (1/s) = 0.0071 (TA); KD = 4.33×10^{-6} M; k_{on} (1/Ms) = 3991.0; k_{off} (1/s) = 0.0173 (PGG); KD = 1.18×10^{-6} M; k_{on} (1/Ms) = 2657; k_{off} (1/s) = 0.0031 (GA); KD = 5.27×10^{-5} M; k_{on} (1/Ms) = 1874.0; k_{off} (1/s) = 0.0988 (UB); KD = 3.59×10^{-6} M; k_{on} (1/Ms) = 661.8; k_{off} (1/s) = 0.0024 (PYG)	[64]
Suramin and quinacrine (1.297.29 and 399.957 g/mol, respectively; treatment of protozoal infection)	Binding affinity to 3CLpro	Biacore T200 instrument (GE Healthcare, Uppsala, Sweden)	KD = 59.7 μ M (suramin) and KD = 227.9 μ M (quinacrine) (k_{on} and k_{off} values N/A)	[65]
Teicoplanin (1709.4 g/mol; glycopeptide antibiotic)	Binding affinity to 3CLpro	Biacore 3000 (GE Healthcare.)	KD = 1.6 mM k_{on} (1/Ms) = 7.8×10^3 ; k_{off} (1/s) = 0.012	[66]
Cobicistat and cangrelor and denufosol (776.023, 776.35 and 773.323 g/mol, respectively; pulmonary diseases)	Binding affinity to 3CLpro	BIAcore-3000 (Biacore Inc., Uppsala, Sweden)	KD = 2.1×10^{-6} M (cobicistat); KD = 6.4×10^{-4} M (cangrelor); KD = 1.4×10^{-3} M (denufosol) (k_{on} and k_{off} values N/A)	[67]
Nonpeptide inhibitors (compounds Z1244904919 and Z1759961356, MW and common uses N/A)	Binding affinity to 3CLpro	Biacore 8K device (Cytiva, Previously GE Healthcare Life Sciences)	KD = 465 μ M (Z1244904919); KD = 133 μ M (Z1244904919) (k_{on} and k_{off} values N/A)	[62]

MW: Molecular weight; k_{on} = association rate; k_{off} = dissociation rate; KD = equilibrium dissociation constants; N/A = not available; TCM: traditional Chinese medicine.

3.2.1. SPR Analysis of Mpro Inhibitors from Plant Origin

Amongst the different ways to develop new drugs, the selection of natural compounds from plants offers a promising approach to obtaining potential drug candidates. In this context, the functionality of SPR biosensors is mainly limited to the monitoring of binding interaction between the target compound and the immobilized protein. Following this detection scheme, Du et al. determined the inhibitory activity of active ingredients derived from TCMs against SARS-CoV-2 3CLpro [63]. Screening of active ingredients through network pharmacology and molecular docking resulted in the selection of seven compounds that were responsible for three TCMs. Particularly, SPR studies revealed high binding affinities of 3CLpro to quercetin (1.24 μM), luteolin (1.63 μM), kaempferol (1.70 μM), naringenin (2.87 μM), and epigallocatechin-3-gallate (6.17 μM) (Figure 10). The best inhibitory effect was further examined by fluorescence resonance energy transfer (FRET)-based cleavage assay, showing that epigallocatechin-3-gallate (EGCG) has the lowest median inhibitory concentration (IC₅₀) value (0.847 μM). Therefore, SPR assays contributed to elucidate the effect of EGCG, an active ingredient abundant in tea plants, for inhibiting the enzymatic activity of 3CLpro.

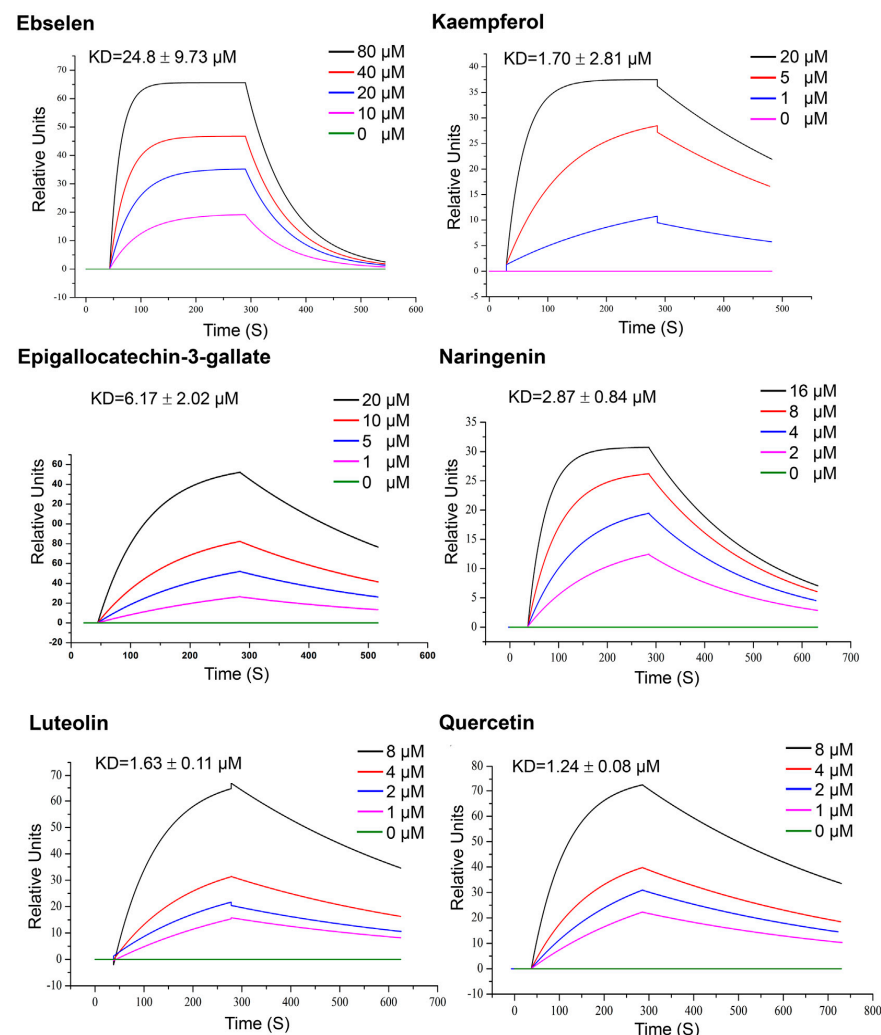


Figure 10. SPR assay of specific binding affinities of several active compounds to immobilized 3CLpro of SARS-CoV-2. Different concentrations of the compounds (1–80 μM) were injected separately on the surface of the ligand chip, and the analyte was sampled at 20 $\mu\text{L}/\text{min}$. The binding time of the analyte to the ligand was 240 s; and the natural dissociation was carried out for 180 s. Data are representative of three independent experiments. Reprinted with permission from Du et al. [63] Copyright © 2021 Elsevier.

A similar approach made use of phenolic compounds to test their anti-SARS-CoV-2 Mpro activity [64]. This study offers an interesting procedure comprising the combination of enzyme inhibition, SPR-, and docking-based assays to evaluate the inhibition capacity of dietary tannins (ellagitannins (punicalagin: PA and ellagic acid: EA) and gallotannins (tannic acid: TA, pentagalloyl glucose: PGG, ginnalin A and gallic acid: GA), and their gut microbial metabolites, urolithins UB and pyrogallol PYG. The optimization of the SPR conditions include the analysis of binding parameters, flow rate and regeneration buffers. Ellagitannins PA and EA showed high binding affinity to the SARS-CoV-2 Mpro protein with K_D values of 6.8×10^{-6} and 2.7×10^{-6} M, respectively. Similarly, gallotannins TA, PGG and GA also exhibited a strong binding capacity with high K_D values of 1.13, 4.33 and 1.18×10^{-6} M, respectively. Lastly, K_D of UB and PYG were 5.27×10^{-5} and 3.59×10^{-6} M, respectively. Although SPR experiments could not predict the specific binding to the catalytic or allosteric domain to the protein, this work demonstrated that biochemical assays, biophysical-based binding assays, and computational approach can be combined successfully for evaluating the inhibition and binding affinities of drug candidates.

3.2.2. Discovery of Mpro Inhibitors via Drug Repurposing

Another way to obtain antiviral drugs relies on the identification of the inhibitory effect of small molecules on 3CLpro protein by repurposing clinically approved drugs. From this perspective, several antiparasitic drugs have demonstrated their antiviral activity against SARS-CoV-2 in cell cultures. In this sense, the inhibitory effect of chloroquine, quinacrine and suramin for blocking SARS-CoV-2 3CLpro has been recently studied by Eberle et al. [65]. Since chloroquine did not affect the SARS-CoV-2 3CLpro activity, SPR biosensing was used to probe the interaction between both suramin and quinacrine with SARS-CoV-2 3CLpro immobilized on the sensor chip. Suramin exhibited stronger interactions with SARS-CoV-2 than quinacrine, exhibiting equilibrium dissociation constants of 59.7 ± 4.5 mM and 227.9 ± 7.9 mM for suramin and quinacrine, respectively. These results were confirmed by molecular docking and MD simulation, indicating that quinacrine blocks the active site entrance through hydrophobic interactions while suramin induces conformational changes in the protein due to allosteric interactions. Additionally, the cooperative effect of suramin and quinacrine to inhibit SARS-CoV-2 3CLpro was evaluated by fluorescence spectroscopy and SPR. SPR experiments indicated that the affinity of quinacrine increased significantly from 230 to 30 mM after the interaction of suramin with SARS-CoV-2 3CLpro, thereby suggesting that suramin binding facilitates quinacrine interaction through a structural change in one active site in the dimer.

Following the same strategy, the effect of teicoplanin, a glycopeptide antibiotic used in the treatment of infections caused by gram-positive bacteria was evaluated as a potential inhibitor of SARS-CoV-2 3CLPro [66]. Protein–drug interactions were examined by SPR involving the immobilization of the 3CLPro protein on the sensor chip and the teicoplanin drug as analyte. The binding affinity was good showing an K_D value of 1.6×10^{-6} M. SPR studies also suggest that 1:1 binding occurred at lower teicoplanin concentrations, whereas the saturation level was not reached when increasing teicoplanin concentration, thus indicating possible nonspecific bindings. Overall, the main asset of this work is the demonstration of the reduction of proteolytic activity of 3CLPro. Although these results were confirmed by molecular docking studies and ThermoFluor[®] Assay, SPR measurements were limited to the analysis of the bimolecular interaction between 3CLPro and Teicoplanin.

Other studies have taken advantage of computational methods to screen approved drugs in search of potential inhibitors against Mpro. For example, Gupta et al. validated the effect of three FDA-approved compounds, cobicistat, cangrelor and denufosol [67]. The latter one was identified from the Drug Bank, while the other two had been previously tested. Biochemical studies were carried out to perform the binding analysis, whereas molecular interactions were evaluated by SPR sensing. The dissociation constants (K_D) of cobicistat, cangrelor and denufosol were 2.1×10^{-6} , 6.4×10^{-4} , and 1.4×10^{-3} M,

respectively, being in agreement with the values of the binding free energy values. The inhibitory effect was examined *in vitro* by enzyme activity and the results validated by biochemical studies. Since cobicistat is already an approved drug for treating HIV infection and a clinical trial is underway to prove its efficiency against COVID-19 disease, further investigation is needed to consider these compounds as therapeutic options against SARS-CoV-2 infection.

Finally, Yang et al. evaluated 49 compounds obtained by multiple conformational-based virtual screening from a protein mimetics library with 8960 compounds [62]. SPR analysis examined the binding profile of the selected candidates showing that six compounds could bind to Mpro. Subsequently, the alteration of the enzyme biochemical function was studied by fluorescence resonance energy transfer assay and bioluminescence resonance energy transfer (BRET) to investigate the inhibition activities against the cell lines of SARS-CoV-2 Mpro. Although the values of dissociation constants were not shown, SPR contributed to the selection of the compounds with potential inhibitory activity.

4. Conclusions and Future Perspectives

This work compiles recent advancements on the discovery of SARS-CoV2 inhibitors by SPR analysis. One of the major benefits of SPR biosensing is the possibility of easily investigating molecular interactions. Owing to this quality, SPR biosensor technology has become a first-line tool for analyzing the binding properties of potential drug candidates against COVID-19.

Primarily, SPR biosensors have been used to measure the binding affinities between an immobilized protein and the selected compound with antiviral properties. Most of the SPR approaches follow this route to characterize the binding specificity between interactants. Recent progress in SPR technology has enabled the detection of weak interactions occurring between small molecules and immobilized proteins with equilibrium dissociation constants in the mM range. In general, SPR-based assays make use of the immobilization of either ACE2 receptor expressed on the membrane of host cells or the main protease Mpro. By utilizing this detection scheme, SPR biosensors are capable of generating a full kinetic profile of the interaction with SARS-CoV2 entry inhibitors. When monitoring drug-ACE2 binding constants, SPR experiments usually focused on the capacity of the antiviral compound to block the interaction with the RBD of the virus spike protein. Alternatively, Mpro-based immobilization formats addressed drug discovery from the perspective of the inhibitory compound ability to prevent virus replication and disrupt the virus life cycle.

In both cases, target molecules subjected to SPR analysis commonly come from natural origin, mainly fruits and vegetables, or pharmaceutical drug synthesis. Among the latter, commercially approved drugs are normally selected for drug repurposing studies according to previously reported therapeutic uses. Thus, a broad range of compounds, including antiparasitic, antibiotics or antipsychotic drugs, have been repositioned as possible anti-COVID 19 drug candidates. Following this path, the principal role of SPR biosensors relies on the recognition of drug targets that can interact with ACE2 receptors of infected cells or inhibit the S protein and MPro main protease of coronaviruses.

The identification of both natural compounds and authorized drugs requires the development of highly specialized biophysical methods. Although SPR configurations are perfectly suited for the screening of small molecules, the number of SPR applications in fragment-based drug discovery is still limited. SPR analysis can provide rapid and sensitive measurements with high selectivity and low protein consumption. Additionally, SPR biosensing can neutralize mass transport effects derived from protein immobilization thanks to the rapid dissociation and the low molecular weight of the analytes. Despite these remarkable advantages, several limitations may arise from the calculation of binding constants due to the low solubility of compounds, thereby requiring previous calibration in the solvent buffer. The multiplexing capacity is also lower in SPR devices in comparison with other biophysical methods such as NMR or X-ray crystallography. However, this limi-

tation can be easily overcome by the low time of response of SPR biosensors. The structural information on binding sites can also be obtained by using competitive assay formats.

Overall, SPR biosensors seem to offer a single methodology for attaining full kinetic profiles while providing the screening of fragment libraries and the validation of fragment hits. Nevertheless, to date, the complementarity with other biophysical methods is unquestionable since NMR produces highly sensitive detection of binding sites and validation whereas X-ray crystallization contributes to select the optimal candidates for fragment enhancement. Consequently, the consolidation of SPR devices as primary screening methods depends on the reduction of false positive/negative rates as well as the optimization of the protein immobilization conditions to obtain the maximum binding response. By addressing these gaps, the new generation of SPR biosensors could achieve the throughput detection of virus entry inhibitors in a timeframe of only a few days.

Author Contributions: E.M. contributed to the conceptualization, methodology, formal analysis, investigation, writing—review and editing and supervision of this work. L.M.L. contributed to the conceptualization and supervision of this work. All authors have read and agreed to the published version of the manuscript.

Funding: This research received no external funding.

Institutional Review Board Statement: Not applicable.

Informed Consent Statement: Not applicable.

Data Availability Statement: Data will be available upon reasonable request to corresponding author.

Conflicts of Interest: The authors declare no conflict of interest.

References

1. Hu, B.; Guo, H.; Zhou, P.; Shi, Z.-L. Characteristics of SARS-CoV-2 and COVID-19. *Nat. Rev. Microbiol.* **2021**, *19*, 141–154. [[CrossRef](#)] [[PubMed](#)]
2. Pattnaik, G.P.; Chakraborty, H. Entry Inhibitors: Efficient Means to Block Viral Infection. *J. Membr. Biol.* **2020**, *253*, 425–444. [[CrossRef](#)] [[PubMed](#)]
3. Sokolova, A.S.; Putilova, V.P.; Yarovaya, O.I.; Zybina, A.V.; Mordvinova, E.D.; Zaykovskaya, A.V.; Shcherbakov, D.N.; Orshanskaya, I.R.; Sinegubova, E.O.; Esaulkova, I.L.; et al. Synthesis and Antiviral Activity of Camphene Derivatives against Different Types of Viruses. *Molecules* **2021**, *26*, 2235. [[CrossRef](#)]
4. Vigant, F.; Santos, N.C.; Lee, B. Broad-Spectrum Antivirals against Viral Fusion. *Nat. Rev. Microbiol.* **2015**, *13*, 426–437. [[CrossRef](#)] [[PubMed](#)]
5. Kumar, P.K.R. Systematic Screening of Viral Entry Inhibitors Using Surface Plasmon Resonance. *Rev. Med. Virol.* **2017**, *27*, e1952. [[CrossRef](#)]
6. Wang, Q.; Liu, Z. Recent Progress of Surface Plasmon Resonance in the Development of Coronavirus Disease-2019 Drug Candidates. *Eur. J. Med. Chem. Rep.* **2021**, *1*, 100003. [[CrossRef](#)]
7. Brouwer, P.J.M.; Caniels, T.G.; van der Straten, K.; Snitselaar, J.L.; Aldon, Y.; Bangaru, S.; Torres, J.L.; Okba, N.M.A.; Claireaux, M.; Kerster, G.; et al. Potent Neutralizing Antibodies from COVID-19 Patients Define Multiple Targets of Vulnerability. *Science* **2020**, *369*, 643–650. [[CrossRef](#)]
8. Shepherd, C.A.; Hopkins, A.L.; Navratilova, I. Fragment Screening by SPR and Advanced Application to GPCRs. *Prog. Biophys. Mol. Biol.* **2014**, *116*, 113–123. [[CrossRef](#)]
9. Congreve, M.; Rich, R.L.; Myszkowski, D.G.; Figarola, F.; Siegal, G.; Marshall, F.H. Fragment Screening of Stabilized G-Protein-Coupled Receptors Using Biophysical Methods. *Methods Enzymol.* **2011**, *493*, 115–136. [[CrossRef](#)]
10. Vanwetswinkel, S.; Heetebrij, R.J.; van Duynhoven, J.; Hollander, J.G.; Filippov, D.V.; Hajduk, P.J.; Siegal, G. TINS, Target Immobilized NMR Screening: An Efficient and Sensitive Method for Ligand Discovery. *Chem. Biol.* **2005**, *12*, 207–216. [[CrossRef](#)]
11. Blundell, T.L.; Jhoti, H.; Abell, C. High-Throughput Crystallography for Lead Discovery in Drug Design. *Nat. Rev. Drug Discov.* **2002**, *1*, 45–54. [[CrossRef](#)] [[PubMed](#)]
12. Duong-Thi, M.-D.; Bergström, M.; Fex, T.; Isaksson, R.; Ohlson, S. High-Throughput Fragment Screening by Affinity LC-MS. *J. Biomol. Screen.* **2013**, *18*, 160–171. [[CrossRef](#)] [[PubMed](#)]
13. Ladbury, J.E.; Klebe, G.; Freire, E. Adding Calorimetric Data to Decision Making in Lead Discovery: A Hot Tip. *Nat. Rev. Drug Discov.* **2010**, *9*, 23–27. [[CrossRef](#)]

14. Kranz, J.K.; Schalk-Hihi, C. Protein Thermal Shifts to Identify Low Molecular Weight Fragments. *Methods Enzymol.* **2011**, *493*, 277–298. [[CrossRef](#)] [[PubMed](#)]
15. Lewis, L.M.; Engle, L.J.; Pierceall, W.E.; Hughes, D.E.; Shaw, K.J. Affinity Capillary Electrophoresis for the Screening of Novel Antimicrobial Targets. *J. Biomol. Screen.* **2004**, *9*, 303–308. [[CrossRef](#)] [[PubMed](#)]
16. Duong-Thi, M.-D.; Meiby, E.; Bergström, M.; Fex, T.; Isaksson, R.; Ohlson, S. Weak Affinity Chromatography as a New Approach for Fragment Screening in Drug Discovery. *Anal. Biochem.* **2011**, *414*, 138–146. [[CrossRef](#)]
17. Kaminski, T.; Gunnarsson, A.; Geschwindner, S. Harnessing the Versatility of Optical Biosensors for Target-Based Small-Molecule Drug Discovery. *ACS Sens.* **2017**, *2*, 10–15. [[CrossRef](#)] [[PubMed](#)]
18. Gauglitz, G. Critical Assessment of Relevant Methods in the Field of Biosensors with Direct Optical Detection Based on Fibers and Waveguides Using Plasmonic, Resonance, and Interference Effects. *Anal. Bioanal. Chem.* **2020**, *412*, 3317–3349. [[CrossRef](#)]
19. Olaru, A.; Bala, C.; Jaffrezic-Renault, N.; Aboul-Enein, H.Y. Surface Plasmon Resonance (SPR) Biosensors in Pharmaceutical Analysis. *Crit. Rev. Anal. Chem.* **2015**, *45*, 97–105. [[CrossRef](#)]
20. Shrivastav, A.M.; Cvelbar, U.; Abdulhalim, I. A Comprehensive Review on Plasmonic-Based Biosensors Used in Viral Diagnostics. *Commun. Biol.* **2021**, *4*, 70. [[CrossRef](#)]
21. Homola, J. Surface Plasmon Resonance Sensors for Detection of Chemical and Biological Species. *Chem. Rev.* **2008**, *108*, 462–493. [[CrossRef](#)]
22. Masson, J.-F. Surface Plasmon Resonance Clinical Biosensors for Medical Diagnostics. *ACS Sens.* **2017**, *2*, 16–30. [[CrossRef](#)]
23. Lin, S.; Shih-Yuan Lee, A.; Lin, C.-C.; Lee, C.-K. Determination of Binding Constant and Stoichiometry for Antibody-Antigen Interaction with Surface Plasmon Resonance. *Curr. Proteom.* **2006**, *3*, 271–282. [[CrossRef](#)]
24. Chavanieu, A.; Pugnère, M. Developments in SPR Fragment Screening. *Expert Opin. Drug Discov.* **2016**, *11*, 489–499. [[CrossRef](#)] [[PubMed](#)]
25. Cao, Y.; Cao, Y.; Shi, Y.; Cai, Y.; Chen, L.; Wang, D.; Liu, Y.; Chen, X.; Zhu, Z.; Hong, Z.; et al. Surface Plasmon Resonance Biosensor Combined with Lentiviral Particle Stabilization Strategy for Rapid and Specific Screening of P-Glycoprotein Ligands. *Anal. Bioanal. Chem.* **2021**, *413*, 2021–2031. [[CrossRef](#)] [[PubMed](#)]
26. Giannetti, A.M. From Experimental Design to Validated Hits a Comprehensive Walk-through of Fragment Lead Identification Using Surface Plasmon Resonance. *Methods Enzymol.* **2011**, *493*, 169–218. [[CrossRef](#)] [[PubMed](#)]
27. Mazzon, M.; Marsh, M. Targeting Viral Entry as a Strategy for Broad-Spectrum Antivirals. *F1000Research* **2019**, *8*. F1000 Faculty Rev-1628. [[CrossRef](#)]
28. Hajduk, P.J.; Greer, J. A Decade of Fragment-Based Drug Design: Strategic Advances and Lessons Learned. *Nat. Rev. Drug Discov.* **2007**, *6*, 211–219. [[CrossRef](#)]
29. Pollack, S.J.; Beyer, K.S.; Lock, C.; Müller, I.; Sheppard, D.; Lipkin, M.; Hardick, D.; Blurton, P.; Leonard, P.M.; Hubbard, P.A.; et al. A Comparative Study of Fragment Screening Methods on the P38 α Kinase: New Methods, New Insights. *J. Comput. Aided Mol. Des.* **2011**, *25*, 677–687. [[CrossRef](#)]
30. Boettcher, A.; Ruedisser, S.; Erbel, P.; Vinzenz, D.; Schiering, N.; Hassiepen, U.; Rigollier, P.; Mayr, L.M.; Woelcke, J. Fragment-Based Screening by Biochemical Assays: Systematic Feasibility Studies with Trypsin and MMP12. *J. Biomol. Screen.* **2010**, *15*, 1029–1041. [[CrossRef](#)]
31. Rouhana, J.; Hoh, F.; Estaran, S.; Henriquet, C.; Boublik, Y.; Kerkour, A.; Trouillard, R.; Martinez, J.; Pugnère, M.; Padilla, A.; et al. Fragment-Based Identification of a Locus in the Sec7 Domain of Arno for the Design of Protein-Protein Interaction Inhibitors. *J. Med. Chem.* **2013**, *56*, 8497–8511. [[CrossRef](#)] [[PubMed](#)]
32. Hulswit, R.J.G.; de Haan, C.A.M.; Bosch, B.-J. Coronavirus Spike Protein and Tropism Changes. *Adv. Virus Res.* **2016**, *96*, 29–57. [[CrossRef](#)] [[PubMed](#)]
33. Pellett, P.E.; Mitra, S.; Holland, T.C. Basics of Virology. *Handb. Clin. Neurol.* **2014**, *123*, 45–66. [[CrossRef](#)]
34. Lan, J.; Ge, J.; Yu, J.; Shan, S.; Zhou, H.; Fan, S.; Zhang, Q.; Shi, X.; Wang, Q.; Zhang, L.; et al. Structure of the SARS-CoV-2 Spike Receptor-Binding Domain Bound to the ACE2 Receptor. *Nature* **2020**, *581*, 215–220. [[CrossRef](#)] [[PubMed](#)]
35. Marks, M.; O'Hara, G.; Houlihan, C.; Bell, L.; Heightman, M.; Hart, N. Severe Acute Respiratory Syndrome Coronavirus 2. *Ref. Modul. Biomed. Sci.* **2021**. [[CrossRef](#)]
36. Hikmet, F.; Méar, L.; Edvinsson, Å.; Micke, P.; Uhlén, M.; Lindskog, C. The Protein Expression Profile of ACE2 in Human Tissues. *Mol. Syst. Biol.* **2020**, *16*, e9610. [[CrossRef](#)] [[PubMed](#)]
37. Lukiw, W.J.; Pogue, A.; Hill, J.M. SARS-CoV-2 Infectivity and Neurological Targets in the Brain. *Cell Mol. Neurobiol.* **2020**, 1–8. [[CrossRef](#)]
38. Zhu, Z.-L.; Qiu, X.-D.; Wu, S.; Liu, Y.-T.; Zhao, T.; Sun, Z.-H.; Li, Z.-R.; Shan, G.-Z. Blocking Effect of Demethylzeylasteral on the Interaction between Human ACE2 Protein and SARS-CoV-2 RBD Protein Discovered Using SPR Technology. *Molecules* **2020**, *26*, 57. [[CrossRef](#)]
39. Day, C.J.; Bailly, B.; Guillon, P.; Dirr, L.; Jen, F.E.-C.; Spillings, B.L.; Mak, J.; von Itzstein, M.; Haselhorst, T.; Jennings, M.P. Multidisciplinary Approaches Identify Compounds That Bind to Human ACE2 or SARS-CoV-2 Spike Protein as Candidates to Block SARS-CoV-2–ACE2 Receptor Interactions. *mBio* **2021**, *12*, e03681-20. [[CrossRef](#)]

40. Xu, H.; Liu, B.; Xiao, Z.; Zhou, M.; Ge, L.; Jia, F.; Liu, Y.; Jin, H.; Zhu, X.; Gao, J.; et al. Computational and Experimental Studies Reveal That Thymoquinone Blocks the Entry of Coronaviruses Into In Vitro Cells. *Infect Dis. Ther.* **2021**, *10*, 483–494. [[CrossRef](#)]
41. Yu, S.; Zhu, Y.; Xu, J.; Yao, G.; Zhang, P.; Wang, M.; Zhao, Y.; Lin, G.; Chen, H.; Chen, L.; et al. Glycyrrhizic Acid Exerts Inhibitory Activity against the Spike Protein of SARS-CoV-2. *Phytomedicine* **2021**, *85*, 153364. [[CrossRef](#)] [[PubMed](#)]
42. Mei, J.; Zhou, Y.; Yang, X.; Zhang, F.; Liu, X.; Yu, B. Active Components in Ephedra Sinica Stapf Disrupt the Interaction between ACE2 and SARS-CoV-2 RBD: Potent COVID-19 Therapeutic Agents. *J. Ethnopharmacol.* **2021**, *278*, 114303. [[CrossRef](#)]
43. Gao, J.; Ding, Y.; Wang, Y.; Liang, P.; Zhang, L.; Liu, R. Oroxylin A Is a Severe Acute Respiratory Syndrome Coronavirus 2-spiked Pseudotyped Virus Blocker Obtained from Radix Scutellariae Using Angiotensin-converting Enzyme II /Cell Membrane Chromatography. *Phytother. Res.* **2021**, *35*, 3194–3204. [[CrossRef](#)] [[PubMed](#)]
44. Binette, V.; Côté, S.; Haddad, M.; Nguyen, P.T.; Bélanger, S.; Bourgault, S.; Ramassamy, C.; Gaudreault, R.; Mousseau, N. Corilagin and 1,3,6-Tri- O -Galloyl- β - D -Glucose: Potential Inhibitors of SARS-CoV-2 Variants. *Phys. Chem. Chem. Phys.* **2021**, *23*, 14873–14888. [[CrossRef](#)] [[PubMed](#)]
45. Singh, S.K.; Singh, S.; Singh, R. Targeting Novel Coronavirus SARS-CoV-2 Spike Protein with Phytoconstituents of Momordica Charantia. *J. Ovarian Res.* **2021**, *14*, 126. [[CrossRef](#)]
46. Ge, S.; Wang, X.; Hou, Y.; Lv, Y.; Wang, C.; He, H. Repositioning of Histamine H1 Receptor Antagonist: Doxepin Inhibits Viropexis of SARS-CoV-2 Spike Pseudovirus by Blocking ACE2. *Eur. J. Pharmacol.* **2021**, *896*, 173897. [[CrossRef](#)]
47. Ge, S.; Lu, J.; Hou, Y.; Lv, Y.; Wang, C.; He, H. Azelastine Inhibits Viropexis of SARS-CoV-2 Spike Pseudovirus by Binding to SARS-CoV-2 Entry Receptor ACE2. *Virology* **2021**, *560*, 110–115. [[CrossRef](#)]
48. Hou, Y.; Ge, S.; Li, X.; Wang, C.; He, H.; He, L. Testing of the Inhibitory Effects of Loratadine and Desloratadine on SARS-CoV-2 Spike Pseudotyped Virus Viropexis. *Chem.-Biol. Interact.* **2021**, *338*, 109420. [[CrossRef](#)]
49. Wang, N.; Han, S.; Liu, R.; Meng, L.; He, H.; Zhang, Y.; Wang, C.; Lv, Y.; Wang, J.; Li, X.; et al. Chloroquine and Hydroxychloroquine as ACE2 Blockers to Inhibit Viropexis of 2019-nCoV Spike Pseudotyped Virus. *Phytomedicine* **2020**, *79*, 153333. [[CrossRef](#)]
50. Lu, J.; Hou, Y.; Ge, S.; Wang, X.; Wang, J.; Hu, T.; Lv, Y.; He, H.; Wang, C. Screened Antipsychotic Drugs Inhibit SARS-CoV-2 Binding with ACE2 in Vitro. *Life Sci.* **2021**, *266*, 118889. [[CrossRef](#)]
51. Cheng, H.; Lear-Rooney, C.M.; Johansen, L.; Varhegyi, E.; Chen, Z.W.; Olinger, G.G.; Rong, L. Inhibition of Ebola and Marburg Virus Entry by G Protein-Coupled Receptor Antagonists. *J. Virol.* **2015**, *89*, 9932–9938. [[CrossRef](#)] [[PubMed](#)]
52. Xu, W.; Xia, S.; Pu, J.; Wang, Q.; Li, P.; Lu, L.; Jiang, S. The Antihistamine Drugs Carbinoxamine Maleate and Chlorpheniramine Maleate Exhibit Potent Antiviral Activity Against a Broad Spectrum of Influenza Viruses. *Front. Microbiol.* **2018**, *9*, 2643. [[CrossRef](#)] [[PubMed](#)]
53. Mercurio, N.J.; Yen, C.F.; Shim, D.J.; Maher, T.R.; McCoy, C.M.; Zimetbaum, P.J.; Gold, H.S. Risk of QT Interval Prolongation Associated With Use of Hydroxychloroquine with or without Concomitant Azithromycin Among Hospitalized Patients Testing Positive for Coronavirus Disease 2019 (COVID-19). *JAMA Cardiol.* **2020**, *5*, e201834. [[CrossRef](#)] [[PubMed](#)]
54. Hewlett, I.; Lee, S.; Molnar, J.; Foldeak, S.; Pine, P.S.; Weaver, J.L.; Aszalos, A. Inhibition of HIV Infection of H9 Cells by Chlorpromazine Derivatives. *J. Acquir. Immune Defic. Syndr. Hum. Retrovirol.* **1997**, *15*, 16–20. [[CrossRef](#)]
55. Walker, S.N.; Chokkalingam, N.; Reuschel, E.L.; Purwar, M.; Xu, Z.; Gary, E.N.; Kim, K.Y.; Helble, M.; Schultheis, K.; Walters, J.; et al. SARS-CoV-2 Assays To Detect Functional Antibody Responses That Block ACE2 Recognition in Vaccinated Animals and Infected Patients. *J. Clin. Microbiol.* **2020**, *58*, 13. [[CrossRef](#)]
56. Ebihara, T.; Masuda, A.; Takahashi, D.; Hino, M.; Mon, H.; Kakino, K.; Fujii, T.; Fujita, R.; Ueda, T.; Lee, J.M.; et al. Production of ScFv, Fab, and IgG of CR3022 Antibodies Against SARS-CoV-2 Using Silkworm-Baculovirus Expression System. *Mol. Biotechnol.* **2021**, *63*, 1223–1234. [[CrossRef](#)]
57. Ravichandran, S.; Coyle, E.M.; Klenow, L.; Tang, J.; Grubbs, G.; Liu, S.; Wang, T.; Golding, H.; Khurana, S. Antibody Signature Induced by SARS-CoV-2 Spike Protein Immunogens in Rabbits. *Sci. Transl. Med.* **2020**, *12*, eabc3539. [[CrossRef](#)]
58. Ye, G.; Gallant, J.; Zheng, J.; Massey, C.; Shi, K.; Tai, W.; Odle, A.; Vickers, M.; Shang, J.; Wan, Y.; et al. The Development of Nanosota-1 as Anti-SARS-CoV-2 Nanobody Drug Candidates. *eLife* **2021**, *10*, e64815. [[CrossRef](#)]
59. Dai, W.; Zhang, B.; Jiang, X.-M.; Su, H.; Li, J.; Zhao, Y.; Xie, X.; Jin, Z.; Peng, J.; Liu, F.; et al. Structure-Based Design of Antiviral Drug Candidates Targeting the SARS-CoV-2 Main Protease. *Science* **2020**, *368*, 1331–1335. [[CrossRef](#)]
60. Zhang, L.; Lin, D.; Sun, X.; Curth, U.; Drosten, C.; Sauerhering, L.; Becker, S.; Rox, K.; Hilgenfeld, R. Crystal Structure of SARS-CoV-2 Main Protease Provides a Basis for Design of Improved α -Ketoamide Inhibitors. *Science* **2020**, *368*, 409–412. [[CrossRef](#)]
61. Hilgenfeld, R. From SARS to MERS: Crystallographic Studies on Coronaviral Proteases Enable Antiviral Drug Design. *FEBS J.* **2014**, *281*, 4085–4096. [[CrossRef](#)]
62. Yang, J.; Lin, X.; Xing, N.; Zhang, Z.; Zhang, H.; Wu, H.; Xue, W. Structure-Based Discovery of Novel Nonpeptide Inhibitors Targeting SARS-CoV-2 M^{Pro}. *J. Chem. Inf. Model.* **2021**, *61*, 3917–3926. [[CrossRef](#)] [[PubMed](#)]
63. Du, A.; Zheng, R.; Disoma, C.; Li, S.; Chen, Z.; Li, S.; Liu, P.; Zhou, Y.; Shen, Y.; Liu, S.; et al. Epigallocatechin-3-Gallate, an Active Ingredient of Traditional Chinese Medicines, Inhibits the 3CLpro Activity of SARS-CoV-2. *Int. J. Biol. Macromol.* **2021**, *176*, 1–12. [[CrossRef](#)] [[PubMed](#)]

64. Li, H.; Xu, F.; Liu, C.; Cai, A.; Dain, J.A.; Li, D.; Seeram, N.P.; Cho, B.P.; Ma, H. Inhibitory Effects and Surface Plasmon Resonance-Based Binding Affinities of Dietary Hydrolyzable Tannins and Their Gut Microbial Metabolites on SARS-CoV-2 Main Protease. *J. Agric. Food Chem.* **2021**, *69*, 12197–12208. [[CrossRef](#)]
65. Eberle, R.J.; Olivier, D.S.; Amaral, M.S.; Gering, I.; Willbold, D.; Arni, R.K.; Coronado, M.A. The Repurposed Drugs Suramin and Quinacrine Cooperatively Inhibit SARS-CoV-2 3CLpro In Vitro. *Viruses* **2021**, *13*, 873. [[CrossRef](#)] [[PubMed](#)]
66. Tripathi, P.K.; Upadhyay, S.; Singh, M.; Raghavendhar, S.; Bhardwaj, M.; Sharma, P.; Patel, A.K. Screening and Evaluation of Approved Drugs as Inhibitors of Main Protease of SARS-CoV-2. *Int. J. Biol. Macromol.* **2020**, *164*, 2622–2631. [[CrossRef](#)]
67. Gupta, A.; Rani, C.; Pant, P.; Vijayan, V.; Vikram, N.; Kaur, P.; Singh, T.P.; Sharma, S.; Sharma, P. Structure-Based Virtual Screening and Biochemical Validation to Discover a Potential Inhibitor of the SARS-CoV-2 Main Protease. *ACS Omega* **2020**, *5*, 33151–33161. [[CrossRef](#)]